DETERMINATION OF TRACE ELEMENT PROVENANCE, RIO LOA BASIN, NORTHERN CHILE

A thesis presented to the faculty of the Graduate School of Western Carolina University in partial fulfillment of the requirements for the degree of Master of Science in Chemistry.

By

Leslie Rae Wilson

Director: Dr. Jerry R. Miller
Whitmire Professor of Environmental Science
Department of Geosciences and Natural Resources

Committee Members: Dr. David J. Butcher, Chemistry and Physics
Dr. Cynthia A. Atterholt, Chemistry and Physics

July 2011

TABLE OF CONTENTS

LIST OF TABLES

LIST OF FIGURES

ABSTRACT

DETERMINATION OF TRACE ELEMENT PROVENANCE, RIO LOA BASIN, NORTHERN CHILE

Leslie Rae Wilson, M.S.

Western Carolina University, (July, 2011)

Director, Dr. Jerry R. Miller

The Atacama Desert, located between the Pacific Ocean and the Andes in northern Chile and southern Peru, is one of the driest regions on the planet. In spite of the extreme aridity, the Atacama is traversed by the Rio Loa, a perennial river which owes its continuous flow to precipitation and runoff at high elevations (>4000 m) along the western Andes, and the emergence of groundwater from thick alluvial aquifers. Water within the Rio Loa is an extremely important resource, but its water and sediment are contaminated, exhibiting levels of trace metals and metalloids that exceed drinking water standards (e.g., for arsenic) and threshold effect guidelines for aquatic biota (e.g., for copper, cadmium, antimony, and zinc). Previous studies, combined with data collected in 2009, suggest that trace metals/metalloids are derived from multiple sources, including El Tatio (a large geyser basin) and three large copper mines. Determination of the relative contribution of contaminants to the river from the geyser basin and the mines has proven problematic using spatial patterns in arsenic concentrations. This study utilizes both total elemental concentrations (arsenic, antimony, copper, and lead) along with isotopes of antimony and lead to distinguish contaminant sources in the Rio Loa. Additionally, a sequential extraction procedure provided additional geochemical understanding of the elemental dispersal pathways via sediment binding.

Isotopes of antimony and lead did not provide enough information to distinguish contaminant sources. Total concentrations of arsenic, antimony, and copper proved to be more

informative, the largest source of copper contamination was determined to be the copper mining operations of El Abra, Radiomiro Tomic, and Chuquicamata. But mining did not input significant quantities of arsenic or antimony, both of which were found in very high concentrations within the Rio Loa. Results showed that El Tatio Geyser Basin input most of the arsenic and antimony contamination. For this reason, a ratio of antimony/copper proved to be a good contaminant tracer to distinguish and quantify contaminated sediment from El Tatio and mining operations. This ratio was applied to floodplain cores and older terrace deposits to determine how sediments have been distributed within the basin over time.

The El Tatio Geyser Basin proved to be the largest contaminator within the Rio Loa basin, mostly due to older terrace deposits, which are high in contamination from El Tatio, continually being eroded and re-worked into the floodplains and channel bed deposits of the lower reaches of the Rio Loa. Contaminated sediment from copper mining operations was not as relevant of a concern because copper transport downstream is inhibited by its adsorption onto Fe-Mn oxide rich particles, which are quickly deposited and/or diluted within the Rio San Salvador (a tributary) before reaching the Rio Loa.

CHAPTER ONE: INTRODUCTION

In the northern region of Chile the Rio Loa traverses the Atacama Desert, which is considered one of the driest places on the planet. The headwaters of the Rio Loa start at high elevations along the western flank of the Andes Mountains and the river flows 440 km westward to the Pacific Ocean (Figure 1). Because of the drainage area's extreme aridity, water derived from the high Andes and delivered downstream through the Rio Loa, is a critical resource used for domestic, agricultural, and industrial purposes. In fact, it provides the primary source of water for the city of Calama (population of approximately 138,000) and for three of the largest copper mines in the world (Chuquicamata, Radomiro Tomic, and El Abra). Unfortunately, the quality of water within the Rio Loa is extremely poor; high concentrations of arsenic (As), antimony (antimony), lithium (Li), boron (B), and other toxic metals and metalloids have been measured within the river's waters throughout much of its course (Romero et al., 2003). Arsenic concentrations, for example, have been observed to exceed the World Health Organizations drinking water standards by a factor of ten (Romero et al., 2003). The health effects of arsenic toxicity are well known and much of the urban water within the Rio Loa is treated for arsenic by iron precipitation at the Cerro Topater water treatment plant before utilized in Calama. However, the water supply for rural communities is not treated and serious health effects due to high arsenic levels have been reported in these areas (Romero et al., 2003).

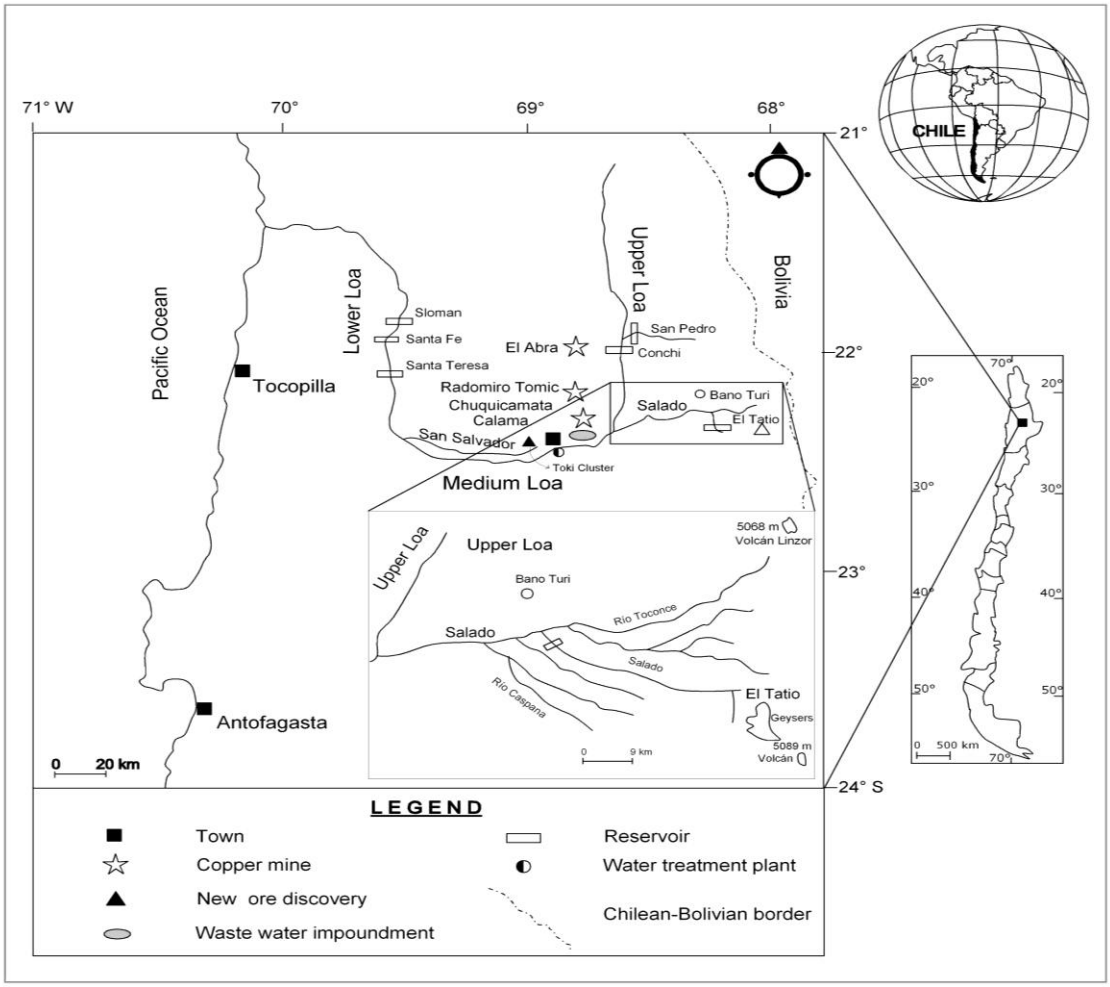

Figure 1: Location map of Study Area

Mining in the Atacama Desert is the source of income for many families and the basis for the local economy of Calama. Open pit mining of the Chuquicamata-Exotica deposit started in the Rio Loa basin in 1923. In 1995, Chuquicamata processed about 150,000 tons of copper sulfides per day (tons/day), 28,000 tons/day copper oxides, and 100,000 tons/day of waste (Romero et al, 2003). Unfortunately, the mining activities within the basin have had significant impacts on water quality and quantity within the Rio Loa. With respect to water quantity, the Chuquicamata mine alone has been known to consume 1760 L of water per ton of mineral processed from the Rio Loa in 1980 (Romero et al., 2003). Today, the consumption rate is

slightly lower because of recycling techniques and long pipelines that bring in desalinated water from the Pacific Ocean. Tailings from mineral processing are currently discharged into the Talabre Impoundment, which is located in a fluvially eroded depression and consists of an area of 40 km^2 (Romero et al., 2003). Prior to the development of the Impoundment in the 1990's, mine tailings were discharged directly into the Rio San Salvador and potentially other drainages in the area.

The other two mines of significance in the area lie along deposits in the porphyry-copper belt and also utilize large quantities of water. These mines, named El Abra and Radomiro Tomic, are located 42 km and 17 km north of Chuquicamata, respectively (Romero et al., 2003). The mined ore deposits lie to the west of a reach of the Rio Loa referred to as the Upper Loa (Figure 2). Alluvial fan deposits located within this upper reach of the Rio Loa valley contain mill and mine tailings from these two mines. The mineral composition of El Abra and Radomiro Tomic deposits are slightly different from that of Chuquicamata. Radomiro Tomic contains minerals higher in sulfides while El Abra is distinguished by having copper-molybdenum rich mineralization (Romero et al., 2003).

Temporally, long-term (decadal) variations in trace metal inputs to the Rio Loa are thought to vary as a function of mining history (methods, production, releases, etc.) at Chuquicamata (starting in 1923), Radomiro Tomic (1970), and El Abra (1996). Following the initial onset of mining, the influence of mine production and processes on contaminant source(s) was probably maximized as tailings were piled in large quantities within the drainages and therefore always available for transport. Thus, significant variations in flux to the river were likely associated with differences in the rainfall runoff patterns responsible for sediment and contaminant entrainment and dispersal.

Spatial patterns in elemental concentrations suggest that high concentrations of arsenic and antimony are also derived from the El Tatio Geyser Field located at the head of the Rio Salado, a tributary to the Rio Loa (Figure 1). The geyser field is around 10 km^2 and discharges between 250-500 L/s of hydrothermal waters into the Rio Salado. Dissolved arsenic concentrations in water from the geyser field are the highest reported for any surficial water body (Landrum et al, 2009). Romero et al., (2003) also argued on the basis of geographical patterns in concentration that the geyser basin is the primary source of arsenic (and other elements) into the Rio Loa Basin. Due to the high concentration of arsenic within the Rio Loa, citizens in towns nearby the river have been affected by water which has arsenic concentrations ranging from 100 to >1000 μg/l. The World Health Organization (WHO) has set the standard arsenic concentration to be no more than 10 μg/l in potable water supplies. The potential for inputs of other metals besides arsenic into the Rio Loa basin from El Tatio is also significant, and there is a definite need to quantify sediment from the El Tatio Geyser Basin.

While stream flows are influenced by groundwater recharge and discharge processes, flow through the drainage network is dominated by surface runoff, which produces high magnitude floods that inundate large areas of the valley floor including much of Calama. Enormous quantities of sediment are transported from the headwater areas and re-deposited downstream during these events. A flood in 2001, estimated to have a recurrence interval of 100-200 years, resulted in the deposition of up to 1 meter of fine-grained sediment over areas exceeding hundreds of km^2 in the basin (Houston, 2006). Smaller, more frequent events, such as those that occurred in 1977, 1997, and 1999 (R.I. > a few decades), have also been shown to inundate large areas and transport large quantities of sediment. However, not all floods are produced by rainfall in the Andes. Flooding may occur over both time scales in response to north-easterly moving frontal storms sourced in the Pacific, which contribute about 30 to 40 percent of the rainfall below 2300 m (Houston, 2006; Rech et al., 2010). Thus, flooding at lower

elevations in the basin may be disconnected from runoff at higher elevations. More importantly, sediment transport and re-deposition appears to be dominated by extreme events as suggested for other basins in arid regions (Baker, 1977).

The effect of the above complexities is that transport and deposition of sediment-borne trace metals/metalloids appears to be dominated by high magnitude runoff events (R.I. > a few decades) that are capable of entraining and transporting large quantities of sediment, and which inundate historic terraces that locally cover large areas of the valley floor (e.g., Calama). Although it is clear that El Tatio and the mines contribute materials to the Rio Loa enriched in trace metals and metalloids, the relative amount derived from each has yet to be quantified and is likely to vary both between events and from one location to another.

The degree of contamination is difficult to assess within the Rio Loa Basin because of the high degree of mineralization in the basin as a whole, and the natural release of trace metals and metalloids during weathering. As a result, determining exactly how much of a particular element is derived from the various anthropogenic and natural sources is a significant problem, which has received considerable attention and must be addressed to effectively manage water quality within the Rio Loa Basin.

Romero et al. (2003) used total arsenic concentrations and chemical speciation data to determine where sediments from El Tatio are being deposited downstream. However, the use of arsenic concentrations to determine source(s) is plagued by analytical complications. More specifically, multiple sources of contamination within the Rio Loa Basin can lead to complex and confusing geographical patterns in concentration. For example, overlapping anthropogenic pollutants can come from both point (mines, and El Tatio), and non-point sources (mineralized rocks), which could show an abrupt increase in contaminant concentration within the river system where these two sources combine. A second problem with the use of total arsenic concentrations

is that arsenic typically possesses a high degree of chemical mobility between the dissolved and particulate forms which can significantly alter spatial patterns.

The geochemical complexities that are involved with elemental and spatial patterns to identify contaminant sources may make the use of arsenic an unreliable predictor for contaminant sources. Physical and geochemical tracers and tracer methods have been growing in popularity to properly identify the sources of contaminants and their transport through the aquatic system to the location where they are currently deposited. A physical or geochemical tracer is usually defined as material from the source location that contains a unique set of characteristics (contaminated or otherwise) that allows it to be distinguished from other constituents in the basin (Miller and Orbock Miller, 2007). Environmental studies utilize a wide range of characteristics unique to each source in the basin to find the best tracer for their purpose. The range of tracer parameters is growing as more methods are being researched and discovered. Some common tracers utilized in environmental studies are sediment grain size and mineralogy, mineral magnetics, acid-soluble trace metals, rare earth elements, and various elemental isotopes.

Isotopes have proven useful in a variety of environmental studies for use as tracers. Isotopes of lead (^{204}Pb, ^{206}Pb, ^{207}Pb, and ^{208}Pb) have been utilized in deciphering the source and dispersal pathways of sediment and sediment borne contaminants in rivers (Miller et al., 2003). To be effective, each source of contaminated sediment should contain different Pb/U to Pb/Th ratios which influence the lead isotopic ratios in the geological material. Problems with this method occur when lead is not associated with, or moving with, contaminated sediment or when lead in the surrounding rocks and the contaminated source materials is from the same source. Isotopes of chromium, molybdenum, copper, zinc, and selenium also hold promise for use as environmental tracers (Miller and Orbock Miller, 2007). Additionally, antimony isotopes have

recently been utilized in environmental applications as tracers and have been proven useful because of their wide range of isotopic values (Rouxel et al., 2003).

The primary objective of this study is to determine the source(s) of selected trace metals and metalloids within alluvial sediments of the Rio Loa, and to determine the relative quantity of these contaminants derived from each source. Inherent in this broad objective is the assessment of the applicability of previously used methods for provenance analysis (e.g., documenting spatial patterns in elemental arsenic concentration). The investigation also explores the use of new methods of source identification based on geochemical speciation and isotopic analysis. More specifically, the study focuses on the ability of lead and antimony isotopes to differentiate anthropogenic mining wastes from natural sediment discharged from El Tatio. Specific hypotheses that were tested during the study include the following: (1) arsenic is a poor tracer due to its high degree of mobility within the basin; (2) lead has a distinct isotopic signature for both mining operations and El Tatio; (3) lead can be utilized as a tracer within the basin; (4) copper input is primarily from mining operations; (5) antimony isotopes are distinct for El Tatio and mining operations; (6) antimony concentration is highest within samples taken from El Tatio; (7) antimony absorbs to silica crystals coming from El Tatio and therefore is found mostly in the residual fraction; (8) antimony isotopes can be used as tracers to determine the source(s) of contaminated sediment; and (9) plots of antimony/copper ratios may be able to distinguish source(s) of contaminated sediment if antimony is high within El Tatio samples and copper is high within mining related samples.

CHAPTER TWO: STUDY AREA

The Rio Loa heads on the western flank of the Andes and flows approximately 440 km downstream across the Atacama Desert to the Pacific Ocean (Figure 2). Rainfall within the basin is highly variable, ranging from approximately 300 mm/yr to above 3000 mm/yr in the Andes to only 1-2 mm/yr near the coast. The basin can be subdivided into seven major geomorphologic areas, which are referred as the Upper Loa, Mine Tributaries (El Abra and Radiomiro Tomic), El Tatio Geyser Field, Rio Salado, the Middle Loa, Rio San Salvador, and the Lower Loa. The Upper Loa extends from the base of the Conchi reservoir in the Andes to its confluence with the Rio Salado (Figure 2). Throughout the reach, the Rio Loa is incised into the underlying rocks, including limestones, rhyolitic and liparitic volcanic deposits, and Miocene to Holocene alluvial and lacustrine deposits. The Rio Salado flows in a westerly direction from a series of geothermal springs called El Tatio Geyser Field in the Andes through volcanic rocks and ultimately to the main stem of the Rio Loa. The Middle Loa represents the reach between the confluence of the Rio Salado and the Rio Loa to the mouth of the Rio San Salvador. The underlying geology along this reach is dominated by Miocene to Holocene alluvial deposits and Pliocene to Holocene evaporitic deposits. The Rio San Salvador is a tributary located downstream of the Chuquicamata copper mine. It eventually enters into the Lower Loa, located after the town of Calama (Figure 2). The Lower Loa flows northward until the river turns sharply to the west and flows through a canyon composed of Mesozoic and Paleozoic sedimentary formations exposed in the Coastal Mountain range (Cordillere de la Costa), located within the middle of the Atacama Desert. Ultimately, the Rio Loa empties into the Pacific Ocean around 22.5˚ latitude, 70.3˚ longitude.

CHAPTER THREE: METHODS

Sampling Methods

Floodplain and Channel Deposits

In early November 2009, sediment and water samples were collected from each of the sample populations. The Rio Loa basin was subdivided into seven geographical areas for sampling on the basis of site geomorphology and potential sources of trace metals to the river. These areas include those mentioned as El Tatio Geyser Field, Rio Salado, Upper Loa, Mine Tributaries of the El Abra and Radiomiro Tomic, Middle Loa, Rio San Salvador, and Lower Loa (Figure 2). Alluvial sediments were collected from within the channel bed (19 samples), floodplain surfaces (13 samples), or terrace deposits (20 samples) (Table 2). Additionally, deposits were sampled at depth from two terraces and three floodplain sites within the middle Rio Loa and Rio Salado. Samples collected from the Upper Loa, upstream of sampling sites RT-1 and RT-2, are thought to primarily represent background concentrations as the reach is located upstream of copper mining operations and input from El Tatio. Contamination from the El Abra and Radomiro Tomic enter the Upper Rio Loa near RT-1 and RT-2 via large alluvial fan channels (Figure 2). Samples from the Rio Salado are downstream of El Tatio Geyser Field and are thought to represent sediment derived from there, while the Rio San Salvador drains contaminants from Chuquicamata copper mine. Sediment located within the Middle Loa is downstream of the confluence of the Rio Salado with the Upper Rio Loa. This section of reach is primarily thought to represent a mixture of sediment from El Tatio and the El Abra and Radiomiro Tomic copper mines. The furthest downstream samples were taken after the confluence of the Rio San Salvador and the Rio Loa, downstream from the town of Calama.

Middle Loa Terrace Deposits

Terrace deposits within sampling sites RL3-T and RL1-T were sampled within the Middle Loa. One sample from each stratigraphic unit within the terrace was collected and analyzed for geochemical data via a total extraction. The RL1-T site was divided into four separate stratigraphic units (A-D) while the RL3-T site was broken into eight separate units (A-H) (Figures 19 and 20).

Sampling Population	Sample names		
El Tatio	**ET-1**	**ET-4**	
	ET-2	**ET-R1**	
	ET-3	**ET-R2**	
El Salado	**RS-1-C**	RS-2-T2	**RS-4-C**
	RS-1-FP	**RS-3-C**	**RS-4-FP1**
	RS-1-T	RS-3-FP (a,b)	**RS-4-FP2**
Upper Loa	**UL-1-C**	**UL-2-FF**	**UL-3-T (a-c)**
	UL-2-C	**UL-3-C**	
		UL-3-FP	
Mine Tributaries	RT-1	RT-2	
Chuquicamata	**RSS-2-1**	**RSS-2T**	
	RSS-2C		
Middle Loa	**RL1-C**	**RL-2-T**	RL-3-FP (a-d)
	RL2-C	RL3-T (a-h)	
	RL1-T (a-d)		
Lower Loa	**RL-4-C**	**RL-4-T**	
	RL-4-FP		

Table 1: Samples associated with each population; samples in bold were analyzed for metal speciation by sequential extraction. See figure 2 for sampling site locations. Channel bed (C), floodplain (FP), and terrace samples (T), along with one sample from a farm field along the floodplain (FF), were sampled during November, 2009.

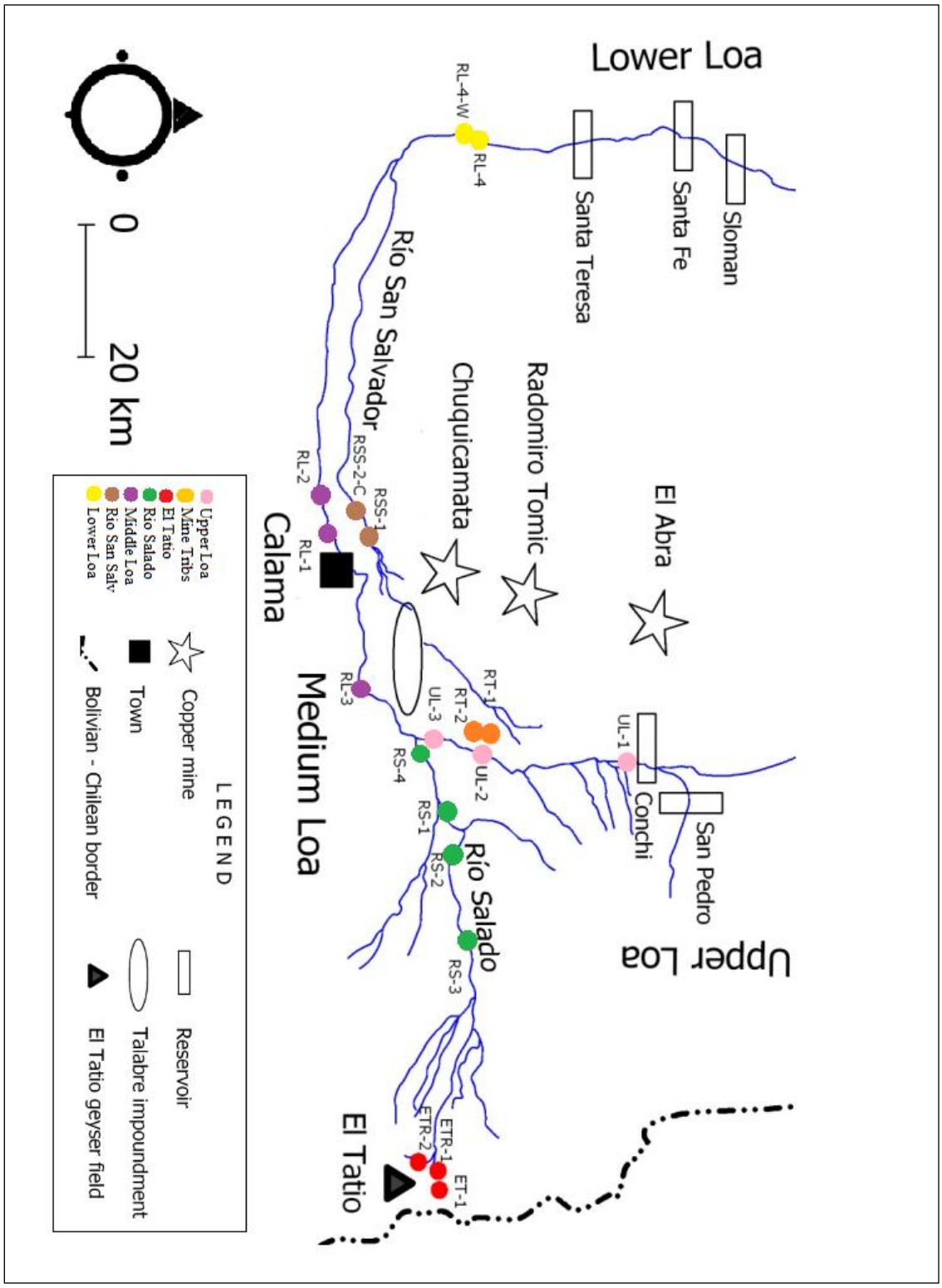

Figure 2: Location map of sample sites. Colors of sample sites indicate how samples were broken up on the basis of geomorphological populations. Refer to legend for population names.

Geochemical Analyses

All of the collected samples were placed in polypropylene sampling containers, packaged in plastics bags, and shipped to the Nevada Bureau of Mines and Geology (NBMG) for analysis. The analysis used to address the objectives included both total and sequential extractions digestion procedures. The elements analyzed in detail were copper, antimony, lead, and arsenic along with isotopes of antimony and lead. The total extraction analysis involved the microwave digestion of 400 mg of dried and homogenized sediment, <2 mm in size, using 4mL of hot Aqua Regia (1:3 ratio of nitric to hydrochloric acid). The samples were analyzed for selected elementals using a Micromass Platform Inductively Coupled Plasma-Mass Spectrometer with a hexapole collision cell (ICP-HEX-MS). With respect to total concentrations, the instrument was calibrated with three USGS (GXR-1, GXR-2, and GXR-5) and two NIST (2709 and 2711) standard reference materials (SRMs). Reagent blanks and the analyte concentrations for the five SRMs were plotted against blank-subtracted integrated peak areas. A regression line was fitted to this array of calibration points and the equation of this line was used to quantify unknown sample concentrations. Deviation of standards from the regression line was used to estimate analytical accuracy, which was +/- 3 to 5 percent of the amount present when determining total concentrations. Accuracy of lead isotopic measurements was assessed with the NIST 981 lead isotope standard. Accuracy was typically better than +/- 0.5 percent, and systematic instrumental bias was corrected. Replicate analyses were used to determine analytical precision, which was < +/- 5 percent.

Sequential Extraction Method

Sequential extraction is a technique which determines how contaminants are bound to sediments, thereby allowing for determination of their mobility and bioavailability (Miller and Orbock Miller, 2007). The analysis was performed on thirty of the fifty collected sediment

samples taken from the Rio Loa Basin (Table 1). One gram of each sample was weighed into a 50 mL centrifuge tube. Wet sample weights were used and later corrected by using sediment moistures measured at 105˚C. A five step sequential extraction was performed on the samples. The strength of the chemical reagent was increased in each step in order to extract various bound fractions from the sediment sample. The exchangeable fraction, carbonate-bound, Fe-Mn oxide metal, organic metal and residual metal fractions were extracted from all thirty samples (Table 2).

Concentrations were determined by first subtracting blank standard responses. Blank samples were run after every fourth sample. An average of the two blanks was calculated and subtracted from sample responses. The subtracted sample response was then divided by the Tm response given by the ICP-HEX-MS instrument. The instrument was calibrated with three USGS (GXR-1, GXR-2, and GXR-5) and two NIST (2709 and 2711) standard reference materials (SRMs). A regression line equation was calculated using Microsoft Office Excel 2007. The regression line equation was then used to determine the concentrations of each sample.

Exchangeable-metal Fraction

The exchangeable fraction used $MgCl_2$ as the chemical reagent. 8 mL of 1 M $MgCl_2$ was added to each sample and agitated frequently at room temperature for 1 hour. Samples were centrifuged for 5 minutes. The aliquot of supernatant was decanted from the leached sediment and 4 mL of Aqua Regia was added to each sample to keep cations from precipitating. 5 mL of supernatant was diluted to 100 mL using nano-pure water. Samples were again diluted 1:4 before they were analyzed by ICP-MS.

Carbonate-Bound Metal Fraction

Remaining residue from the previous sample leach was then extracted with 8 mL of 1 M sodium acetate solution which was adjusted to a pH of 5.00 with acetic acid in order to extract the

carbonate-bound metal fraction. Samples were agitated at room temperature for 5 hours and then centrifuged for 5 minutes. The aliquot of supernatant was decanted and 4 mL of Aqua Regia was added to each sample. 5 mL of supernatant was diluted to 100 mL using nano-pure water. Samples were again diluted 1:4 before they were analyzed by ICP-MS.

Fe-Mn Oxide Metal Fraction

The Fe-Mn oxide metal fraction from each sample was extracted using 20 mL of 0.04 M NH_2OH*HCL and applied to the remaining residue left after the carbonate bound metal fraction leach. The samples were agitated periodically in a boiling water bath for 5 hours and then centrifuged for 5 minutes. The aliquot of supernatant was decanted from the leached material and 4 mL of Aqua Regia was added to each sample. 5 mL of supernatant was diluted to 100 mL using nano-pure water. Samples were again diluted 1:4 before they were analyzed by ICP-MS.

Organic-Metal Fraction

Reagents for the organic metal fraction included 3 mL of 0.02 M HNO_3 and 5 mL of 30% H_2O_2 which was adjusted to a pH 2 with HNO_3. Each sample was agitated periodically at 85˚C for 2 hours. 3 mL of H_2O_2 (pH 2) was added to each sample and agitated periodically on a hot bath at 85˚C for 3 hours. After 3 hours, 5 mL of 3.2 M ammonium acetate in 20% v/v HNO_3 was added to each sample before being agitated periodically again at room temperature for 30 minutes. Samples were centrifuged for 5 minutes. The aliquot of supernatant was decanted from the remaining leached sediment and 4 mL of Aqua Regia was added to each sample. 5 mL of supernatant was diluted to 100 mL using nano-pure water. Samples were again diluted 1:4 before they were analyzed by ICP-MS.

Residual Metal Fraction

Only samples from El Tatio were analyzed for the residual metal fraction (ET-1, ET-2, ET-3, ET-4, ET-R1, and ET-R2). The extraction was performed by adding 10 mL of concentrated HF and 16 mL of Aqua Regia to each sample. The six El Tatio samples were heated on a hot bath for 2 hours while agitating periodically. Samples were centrifuged for 5 minutes. The aliquot of supernatant was decanted from the 50 mL centrifuge tube, and 4 mL of Aqua Regia was added to each. 5 mL of supernatant was diluted to 100 mL using nano-pure water. Samples were again diluted 1:4 before analyzed by ICP-MS. Summing the concentrations of each previous extraction, and then subtracting that value from the total metal concentration determined the residual metal fraction for all other samples.

Total Metal Fraction

Total metal analysis was determined by digesting 400mg of sample with 8 mL Aqua Regia and 2 mL of concentrated HF. Each sample was agitated periodically for 2 hours in a hot bath. The samples were then diluted to 500 mL with nano-pure water before being run through the ICP-MS.

Chemical Species or Form	Reagent Used	Bioavailability
Exchangeable Ions	1M $MgCl_2$	Available
Carbonate Bound Fraction	1M CH_3COONa solution adjusted to a pH of 5.0 with CH_3COOH	Less available: (Ion exchange reactions)
Fe-Mn Oxide Bound Fraction	0.04M NH_2OH*HCL	Less Available; promoted by chemical alteration (Mn oxides/Hydroxides)
Organic Bound Metal Fraction	0.02M HNO_3 with 30% H_2O_2 which has been adjusted to a pH 2 with HNO_3 and 3.2M CH3COONH$_4$ in 20%v/v HNO_3	Available only after chemical alteration (Fe oxides/hydro)
Residual Ions within Crystalline Structure of Minerals	Aqua Regia and Concentrated HF	Unavailable unless severely weathered or decomposed

Table 2: Five-Step Sequential Extraction method used

Antimony Hydride Generation

Previous studies used antimony isotopes as environmental tracers by analyzing seawater samples near hydrothermal vents using a hydride generation apparatus attached to the ICP-MS system (O. Rouxel et al., 2003). Hydride Generation is a technique that helps eliminate spectral and/or isobaric interferences within the ICP-MS to more accurately determine concentrations for certain elements including antimony. Antimony Standards of 10 μg/100 mL, 50 μg/100 mL, and 100 μg/100 mL with 5% HCL were made for the hydride generation trials. Formation of Stibine gas (SbH_3) is formed by injection of a 5% solution of NaBOH combined with a 10% solution of HNO_3 into the sample to react with any antimony present and produce Stibine gas, which then travels through the hydride generation apparatus and into the ICP-MS instrument for measurement. The solutions were made 10 minutes before starting the hydride generation due to likelihood of chemical break down. The apparatus for hydride generation was set up so Stibine gas would be formed and injected directly into the ICP-MS. For trial runs, the antimony standard was placed into a 500 mL round bottom flask while it was injected using a syringe and needle with 10% $NaBH_4$ and 5% NaOH at a slow rate.

This technique worked well while being tested with only standard solutions, but when tried with the samples from the Rio Loa the apparatus did not produce the same reproducible results as previous antimony isotopic studies. That is, chemical interferences and/or matrix effects were produced within the apparatus and values for antimony isotopes were not consistent with previous literature findings. Research into the method proved that the instrument utilized had a hexipole collision cell located before the quadruple mass analyzer of the MS instrument which provided a better detector for antimony isotope samples from the Rio Loa Basin. Because of these findings, total digestions of the samples from within the Rio Loa Basin were run through the ICP-HEX-MS by direct liquid injection and reproducible antimony isotopic values were

detected. Results were examined by plotting ^{123}Sb vs. ^{121}Sb to test how accurate the instrument was measuring.

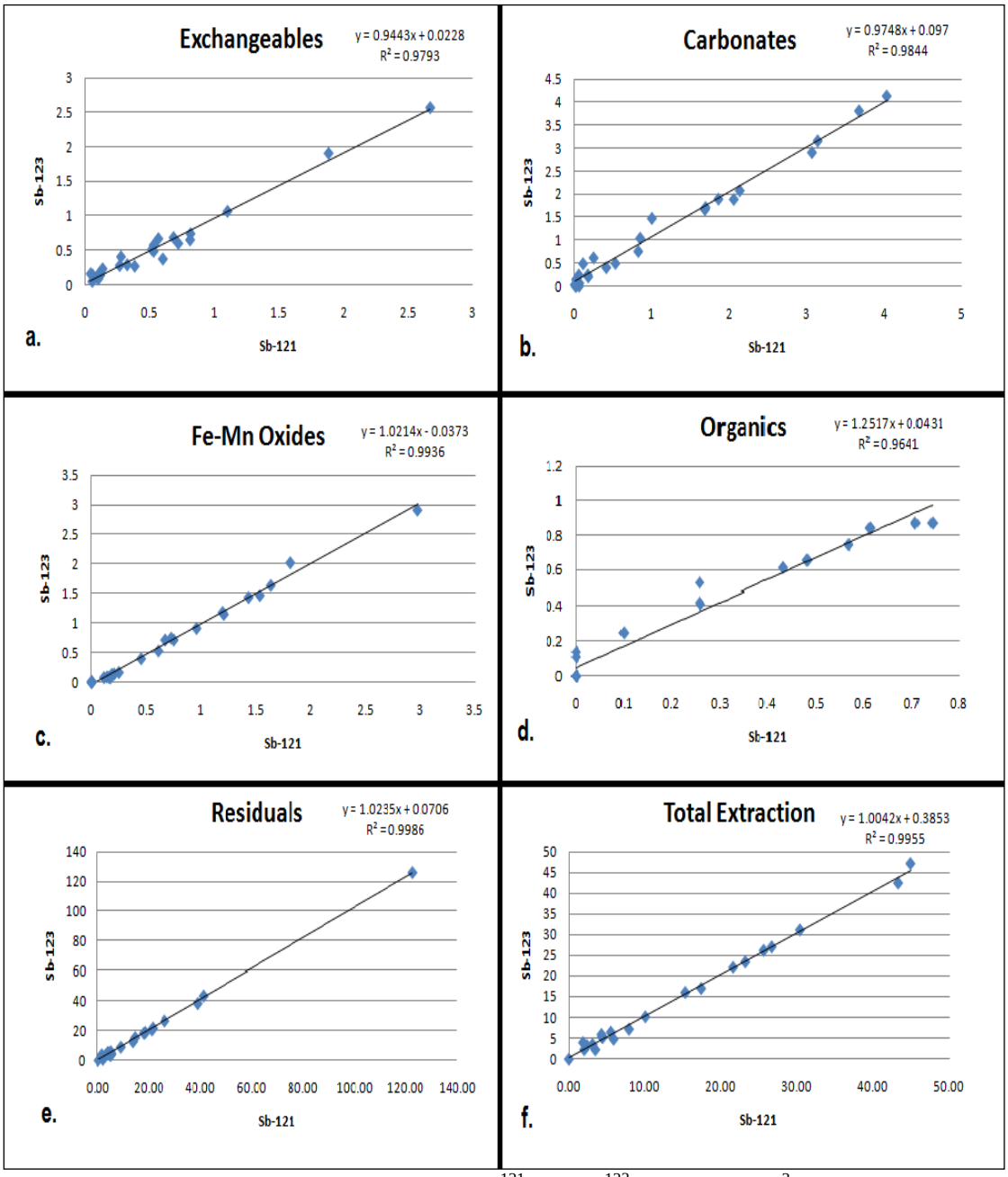

Figure 3: Analytical determination for ^{121}Sb and ^{123}Sb isotopes. R^2 values indicate how accurate the ICP-MS instrument measured antimony isotopes. Lower R^2 values indicate small chemical interferences within the instrument.

CHAPTER FOUR: RESULTS

Comparison of Total Elemental Concentrations to Biotic Effect Guidelines

Total trace metal and metalloid concentrations in sediment samples from the Rio Loa Basin are high with respect to both background and operatic effect guidelines (Table 3). For example, MacDonald et. al. (2000) researched levels in which biota are harmed by toxic trace metals within the channel bed sediment. Their determined levels of effect were subdivided into lower and upper concentrations referred to as the threshold effect concentration (TEC) and the probable effect concentration (PEC). The threshold effect concentration (TEC) refers to a value in which the biota was first noticed to be negatively affected by harmful concentrations of toxic trace metals. The probable effect concentration (PEC) refers to a value where there is a "high probability" that biota living within the environmental system will be harmed by the concentrations of toxic trace metals. The TEC and PEC for selected toxic trace metals are given in Table 3, along with determined data for each sampling population within the Rio Loa Basin. All six sampling populations exhibited concentrations above the threshold and probable effect concentrations for some elements (Table 3). MacDonald did not present data on antimony, but average soil antimony concentrations worldwide are 0.67 ppm (Buonicore et al., 1996). Concentrations found within the Upper Rio Loa, which is upstream of both mining operations and El Tatio, are more than 10 times greater than the average soil data. An increase in this already high background antimony may pose a threat to local biota living within the water column even though it is tolerant of high background concentrations.

The concentrations of selected, toxic trace metals within the Rio Loa Basin exhibit some notable geographical patterns. The El Tatio Geyser Field contains arsenic concentrations which are, on average, 90 times higher than the PEC determined values (Table 3). Additionally, concentrations of antimony are more than 25 times higher within these samples than the other

sample populations. With respect to sediment contaminated by mining operations, alluvium within the Rio San Salvador is above the PEC for arsenic, cadmium, copper, lead, and zinc, and above the TEC for chromium and nickel. Sediment within alluvial fan channels receiving input from the El Abra and Radiomiro Tomic mine tributaries is above the PEC values for arsenic and copper, and above the TEC for cadmium and nickel. Overall, downstream of mining operations (mine tributaries and Rio San Salvador), copper concentrations are the most significant, whereas downstream of El Tatio, arsenic and antimony concentrations are the highest (Table 3).

	Channel Bed Sediment - Concentration (µg/g)- 2009 Data								
Element	**TEC**	**PEC**	**Ave Soil**	**El Tatio**	**Mine Tribs.**	**Upper R. Loa**	**Rio Salado**	**Middle R. Loa**	**R. San Salvador**
Antimony	---	---	0.67	521	9.92	7.84	20.1	7.40	22.4
Arsenic	9.79	33.0	7.2	***2960***	***162***	***34.4***	***496***	***248***	***544***
Cadmium	0.99	4.98	0.06	0.69	*2.30*	*2.17*	*1.80*	*1.03*	***6.64***
Chromium	43.4	111	54	21.6	42.1	*48.4*	30.3	15.2	*55.9*
Copper	31.6	149	25	*55.8*	***726***	*63.7*	*68.9*	16.9	***1580***
Lead	35.8	128	19	15.6	24.2	11.4	9.49	9.58	***154***
Nickel	22.7	48.6	19	5.58	*22.7*	17.4	10.2	7.94	*24.7*
Zinc	121	459	60	44.0	117	74.2	89.0	46.0	***1040***

Table 3: TEC, Consensus based threshold effects conc.; PEC, Probable effects threshold conc. (from MacDonald et al, 2000); The mean concentrations that are red in color are above the probable effect concentration (PEC) and the ones in yellow are above the threshold effect concentration (TEC). Average soils data from Buonicore (1996).

Comparison of Total Concentrations between Sampling Populations

Box and whisker plots for each sampling population were plotted to determine elemental differences among the groups, with regards to lead, arsenic, antimony, and copper surface concentrations. Plots were created using Microsoft Office Excel 2007 and analyzed by observing the total concentrations and ranges of selected elements within each of the population areas of the Rio Loa Basin. Population areas containing high concentrations of selected trace metals and metalloids are assumed to have the most significant input of selected trace metal and metalloid contamination into the Rio Loa Basin.

Statistical analysis was done using R commander version 2.12.1. A one way ANOVA test statistic using pairwise comparisons of means for each element (lead, arsenic, antimony, and copper) and isotopic ratio (antimony and lead) was calculated across the different basin populations for statistical comparisons. Compact letter display (CLD) shows how each population is statistically different from one another by t-test analysis between two separate populations by displaying either an A or B based on the results. In some cases, populations were found to have an "AB" CLD designation, which represents a population which is statistically similar to two separate populations (A and B) within the basin. Results from the t-test between each population for all elements are show in Appendix A. The one way ANOVA test statistic was analyzed at the 95% confidence interval and elements between populations that were below the 0.05 threshold p-value where determined to have populations which were statistically different from one another.

Total lead concentrations (ppm) for each population area within the Rio Loa Basin had overlapping values where one particular input source of lead could not be distinguished. The ANOVA test statistic indicated that the p-value for the population was 0.3123; therefore all the populations were similar throughout the basin (Figure 4). CLD shows that the t-tests between each population were all above the 0.05 p-value and no single population is different from another, indicating that lead is uniformly distributed throughout the Rio Loa Basin (Appendix A). Because no particular input source of lead could be distinguished, total lead concentrations were not utilized for tracer analysis in this study.

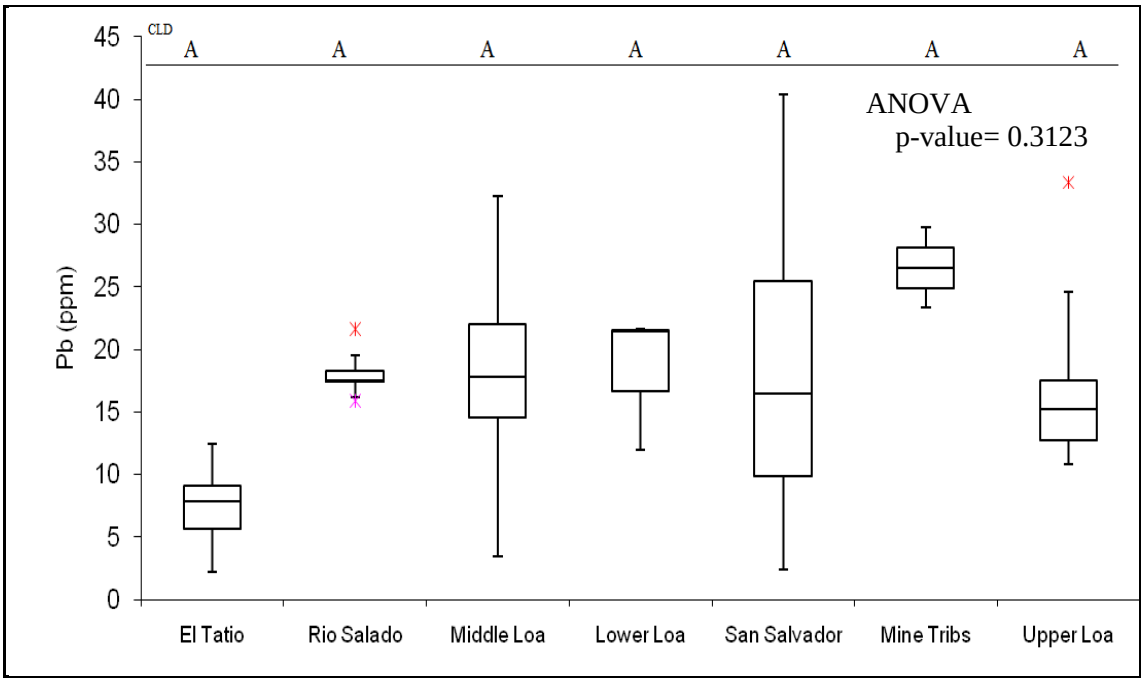

Figure 4: Box and Whisker plot of lead (ppm) for each geomorphologic area with the Rio Loa Basin. Plot show the minimum, maximum, median, upper/lower quartiles, and minimum/maximum outliers. Compact letter display (CLD) shows that all populations are statistically similar.

Labels	El Tatio	Rio Salado	Middle Loa	Lower Loa	San Salvador	Mine Tribs	Upper Loa
Min	2	16	3	12	2	23	11
Q_1	6	17	15	17	10	25	13
Median	8	17	18	21	16	27	15
Q_3	9	18	22	22	26	28	18
Max	12	22	32	22	40	30	33
IQR	3	1	7	5	16	3	5
Upper Outliers	0	1	0	0	0	0	1
Lower Outliers	0	1	0	0	0	0	0

Table 4: Statistical values for lead (ppm) as shown in the box and whisker plot.

Total concentrations of arsenic (ppm) were highest within the samples from El Tatio Geyser Field (Figure 5). Sediment samples from El Tatio had a maximum value of 6422 ppm, a minimum concentration of 1247 ppm, and an IQR of 2386. Samples from the El Tatio Geyser Field had a calculated median arsenic concentration which was between 4 and 5 times higher than

the Rio San Salvador samples, and 13 times higher than the median concentration calculated for the mine tributaries of El Abra and Radiomiro Tomic. The one way ANOVA test determined a p-value of 1.799×10^{-4}, which is significantly below the 0.05 confidence interval indicating a large between population difference within the basin as a whole (Figure 5). CLD indicates El Tatio Geyser Field is a separate population from all other samples within the basin based on the t-tests performed between all population means (Figure 5) (Appendix A). Large differences in the overall arsenic concentrations between the El Tatio samples and the other geomorphologic areas presented on the graph makes the utilization of total arsenic concentration plausible as a geochemical tracer.

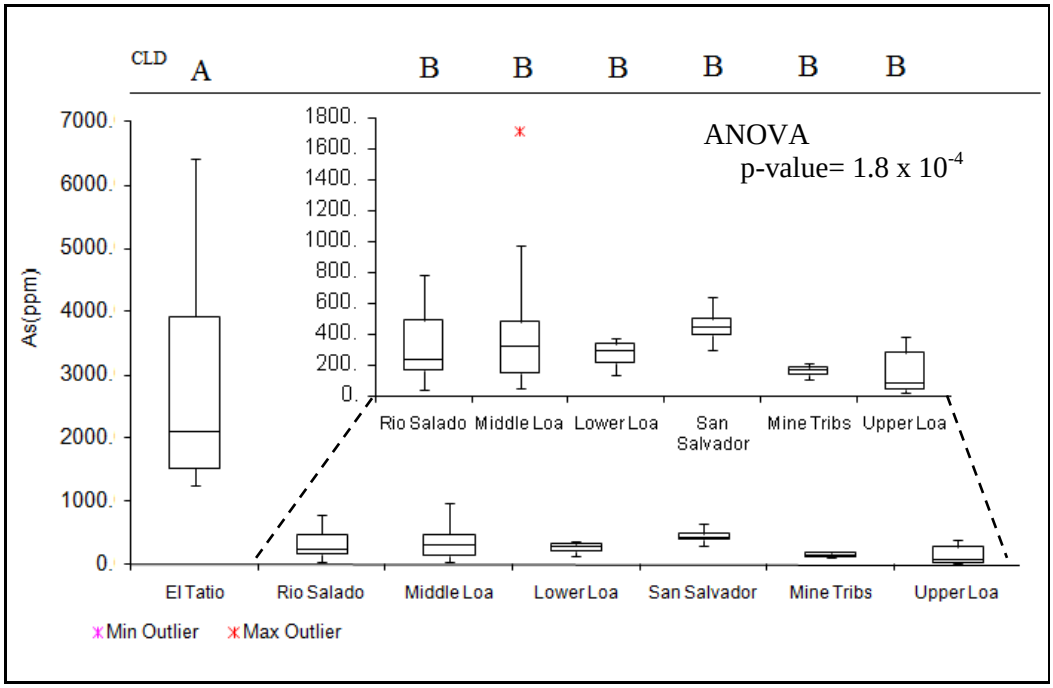

Figure 5: Box and whisker plot of arsenic within each geomorphologic area. Dotted lines represent enlarged section of larger plot. Compact letter display (CLD) shows that El Tatio (A) is statistically different from all other populations (B) based on t-test analysis between populations.

Labels	El Tatio	Rio Salado	Middle Loa	Lower Loa	San Salvador	Mine Tribs	Upper Loa
Min	2.156	0.010	0.000	0.862	0.000	0.000	0.000
Q_1	4.840	0.165	0.361	1.103	0.010	0.003	0.007
Median	5.199	0.264	0.599	1.344	0.014	0.005	0.129
Q_3	15.762	0.384	1.033	1.471	0.076	0.008	0.163
Max	56.430	1.225	1.872	1.599	0.255	0.010	0.248
IQR	10.921	0.218	0.672	0.369	0.066	0.005	0.156
Upper Outliers	1.000	2.000	0.000	0.000	1.000	0.000	0.000
Lower Outliers	0.000	0.000	0.000	0.000	0.000	0.000	0.000

Table 5: Statistical values for box and whisker plot of arsenic.

Similar to total arsenic concentrations, total antimony concentrations were also higher within samples collected from El Tatio relative to the other sample populations (Figure 6). The concentrations of antimony within the El Tatio samples were 2 orders of magnitude higher than all of the other populations within the Rio Loa Basin. Antimony concentrations at El Tatio are between 289-2840 ppm, with a median of 1780 ppm. The one way ANOVA test indicates that there are differences between the populations based on a p-value of 8.35×10^{-4}, which rejects the null hypothesis at the 95% confidence interval. CLD on antimony concentrations results in a similar outcome to arsenic, in that El Tatio is the population which is statistically different from the other populations within the basin (Figure 6) (Appendix A). In comparison of antimony to the mine-related samples, median concentrations are 90 times higher than those analyzed within the Rio San Salvador and 325 times higher than the median antimony concentration observed in the sediment downstream of input from the El Abra and Radiomiro Tomic mining operations (Table 6). Due to the distinct differences in antimony concentrations at the El Tatio Geyser Field compared to the other geomorphologic areas within the Rio Loa Basin, especially sediment from mining operations, the total concentrations of antimony were utilized as a sediment tracer.

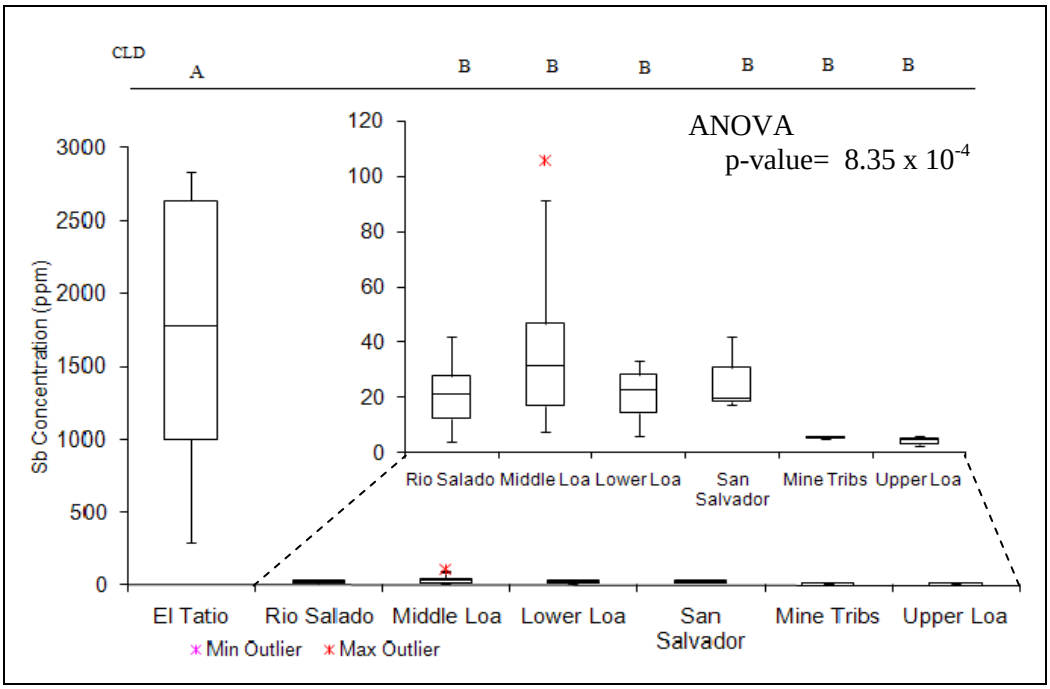

Figure 6: box and whisker plot of antimony concentrations (ppm) for all populations within the Rio Loa Basin. Dotted lines represent enlarged section of the larger graph. Compact letter display (CLD) indicates that El Tatio is a separate population (A) compared to all other populations within the basin (B) based on t-test results between populations.

Labels	El Tatio	Rio Salado	Middle Loa	Lower Loa	San Salvador	Mine Tribs	Upper Loa
Min	289	4	7	6	18	5	2
Q_1	1003	12	17	15	19	5	3
Median	1780	21	32	23	19	5	5
Q_3	2640	28	47	28	31	6	5
Max	2840	42	106	33	42	6	6
IQR	1637	15	30	14	12	0	2
Upper Outliers	0	0	1	0	0	0	0
Lower Outliers	0	0	0	0	0	0	0

Table 6: Statistical values for box and whisker plot of antimony concentrations (ppm)

Figure 7 shows that copper concentrations are high in both the Rio San Salvador samples, found downstream of Chuquicamata, and the alluvial fan samples, that drain the El Abra and Radiomiro Tomic copper mines. The Rio San Salvador samples have a median of 762 ppm while

the samples from the mine tributaries have a median of 726 ppm (Table 7). The inner quartile range (IQR) of the samples within the Rio San Salvador is much higher than those taken from the mine tributaries. The IQR for the Rio San Salvador was calculated to be 1300 ppm, while the IQR for the mine tributaries was calculated to be 172 ppm. In comparison to the El Tatio samples, median copper concentrations within samples from the Rio San Salvador and mine tributaries are between 13 and 14 times greater than the calculated median copper concentration for the El Tatio samples. El Tatio has the lowest minimum concentration of copper, calculated to be 9.8 ppm, while the Lower Loa has the lowest median copper concentration of 19.83 ppm (Table 7). Statistical analyses on the total concentrations of copper indicate that mining operations are different from all other populations within the basin.

A one way ANOVA test throughout the entire basin calculated that there are distinct differences based on a p-value of 1.397×10^{-6}, much below the 0.05 limit at the 95% confidence interval. CLD between populations indicates that the two populations representing mining operations (Chuquicamata and mine tributaries) are the populations which are distinctly different based on t-test results (Figure 7) (Appendix A). Distinct differences in total copper concentrations between mining operations and all other population areas, especially sediment directly downstream of the El Tatio Geyser Field, makes the utilization of total copper concentrations as a contaminated sediment tracer for mining operations plausible.

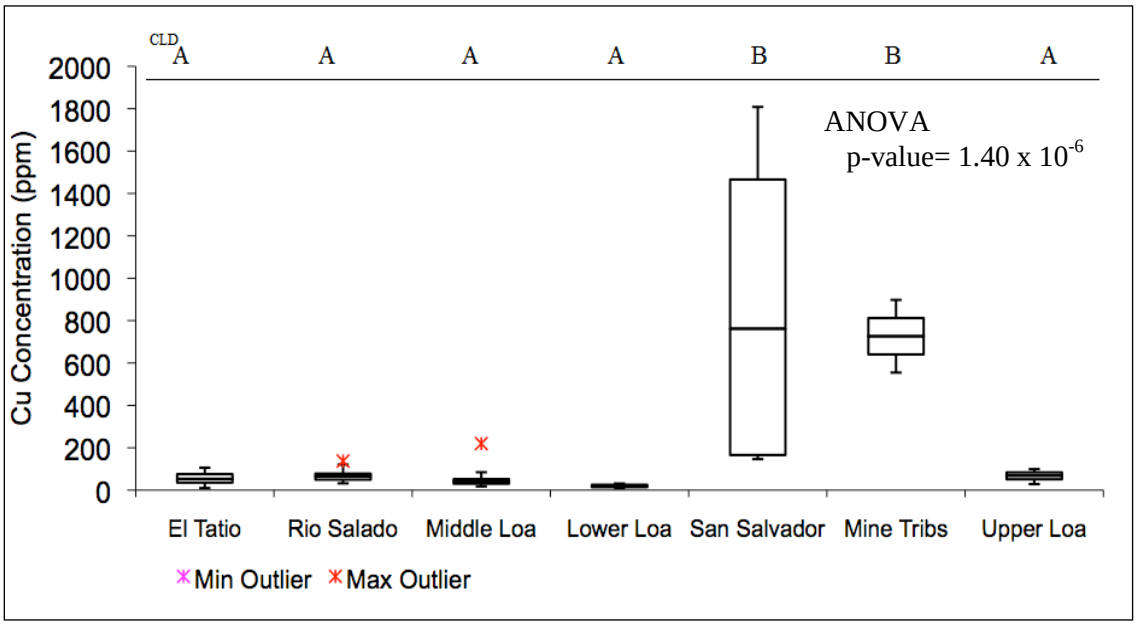

Figure 7: Box and whisker plot of copper concentrations for each population. The box and whisker plot contains the average, upper quartile, lower quartile and both maximum and minimum outliers. CLD shows that the Rio San Salvador and Mine Tributaries are statistically similar.

Labels	El Tatio	Rio Salado	Middle Loa	Lower Loa	San Salvador	Mine Tribs	Upper Loa
Min	10	32	18	10	147	555	28
Q_1	36	50	30	15	166	641	51
Median	53	66	40	20	762	726	68
Q_3	76	78	52	26	1466	812	84
Max	106	137	220	31	1808	898	99
IQR	40	29	22	11	1300	172	33
Upper Outliers	0	1	3	0	0	0	0
Lower Outliers	0	0	0	0	0	0	0

Table 7: Statistical values for box and whisker plot of copper concentrations

Tracer Analysis of the Antimony/Copper Ratio

The copper and antimony data presented above show that their concentrations differ significantly between El Tatio and the copper mines. These large differences suggest that the ratio of antimony/copper will be an effective tracer of contaminated sediment. Thus, antimony/copper

ratios were calculated by dividing the total concentrations of antimony by the total concentrations of copper for each sample to help quantify the amount of contaminated sediment from these two source types (i.e. the mining operations and the El Tatio Geyser Field) (Figure 8).

Samples from the El Tatio Geyser Field had the highest ratio, 56.43 and the largest IQR calculated, 10.92 (Table 8). The lowest ratios calculated were 0.005 and 0.014, represented by the mine tributaries, El Abra and Radiomiro Tomic, and the Rio San Salvador, respectively. The El Tatio samples had a calculated median ratio which was 370 times larger than the median ratio calculated within the Rio San Salvador samples, and more than a 1000 times larger than the median ratio of the mine tributaries. Large error bars within the plots of the Rio Salado, and especially the Middle Loa, represent sediment mixing of input from both the mining operations and the El Tatio Geyser Field (Figure 8).

Statistical analyses done on the antimony/copper ratio indicates that there are differences between populations based on a one way ANOVA test statistic with a p-value of 7.4×10^{-3}. Between populations, the t-tests found that the mean for El Tatio was different from the Rio Salado, Middle Loa, Rio San Salvador, and Upper Loa, but not statistically different from the Lower Loa and the Mine Tributaries. The Lower Loa and Mine Tributaries are statistically similar to El Tatio because the t-test statistics performed between them were calculated to be 0.0783 and 0.1271, respectively (Appendix A). However, they were also determined to be statistically similar to all other populations, based on the CLD designation of "AB", indicating that these populations are similar to both A and B designated populations (Figure 8). Although, statistical error could be present within the Mine Tributary population due a very small sample size of only two samples available when this test was performed.

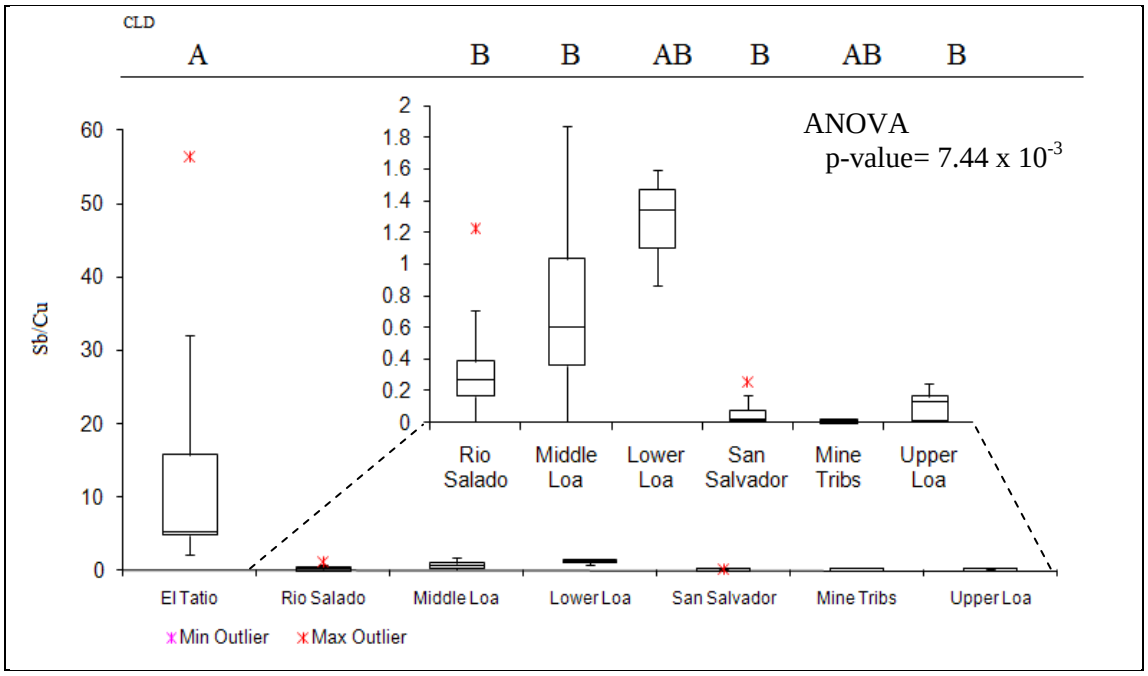

Figure 8: Box and whisker plot of antimony/copper for each population. Compact letter display (CLD) indicates that the Lower Loa and mine tributaries are statistically similar to both El Tatio (A) and all other populations within the Rio Loa (B) based on t-test analysis.

Labels	El Tatio	Rio Salado	Middle Loa	Lower Loa	San Salvador	Mine Tribs	Upper Loa
Min	2.156	0.010	0.000	0.862	0.000	0.000	0.000
Q_1	4.840	0.165	0.361	1.103	0.010	0.003	0.007
Median	5.199	0.264	0.599	1.344	0.014	0.005	0.129
Q_3	15.762	0.384	1.033	1.471	0.076	0.008	0.163
Max	56.430	1.225	1.872	1.599	0.255	0.010	0.248
IQR	10.921	0.218	0.672	0.369	0.066	0.005	0.156
Upper Outliers	1	2	0	0	1	0	0
Lower Outliers	0	0	0	0	0	0	0

Table 8: Statistical values for antimony/copper box and whisker plot

Antimony Isotopic Analysis within the Rio Loa Basin

Antimony isotopic analysis revealed that the background bedrock material located within the Upper Loa was able to be distinguished from both anthropogenic (mining activities) and natural sediment input of toxic metals and metalloids within the lower reaches of the Rio Loa

(Figure 9). However, this method could not distinguish between each source of contamination (i.e. El Tatio and the copper mines) (Figure 9). The mean isotopic signature of antimony within the Upper Loa is larger than both the anthropogenic and natural (El Tatio) hypothesized sources of contamination (Figure 9). Unfortunately, the median antimony signature for both El Tatio and the Rio San Salvador (i.e. Chuquicamata) is similar, with a $^{123}Sb/^{121}Sb$ ratio of around 0.77 and 0.78, respectively (Table 9). The Upper Loa contains a ratio that is higher with a median value of 1.04, and an IQR of 0.110 (Table 9). The mean isotopic signature decreases to 0.78 after the confluence of the Upper Loa and the Rio Salado, and continues to decline moving downstream throughout the Rio Loa system. Statistical analyses confirmed that the Upper Loa is statistically different than all other populations based on t-tests between populations (Appendix A). CLD displays the Upper Loa (B) to be statistically separate from all other populations (A). The one way ANOVA test statistic was calculated to be 1.32×10^{-4}, considerably below the 0.05 threshold p-value for a 95% confidence interval (Figure 9).

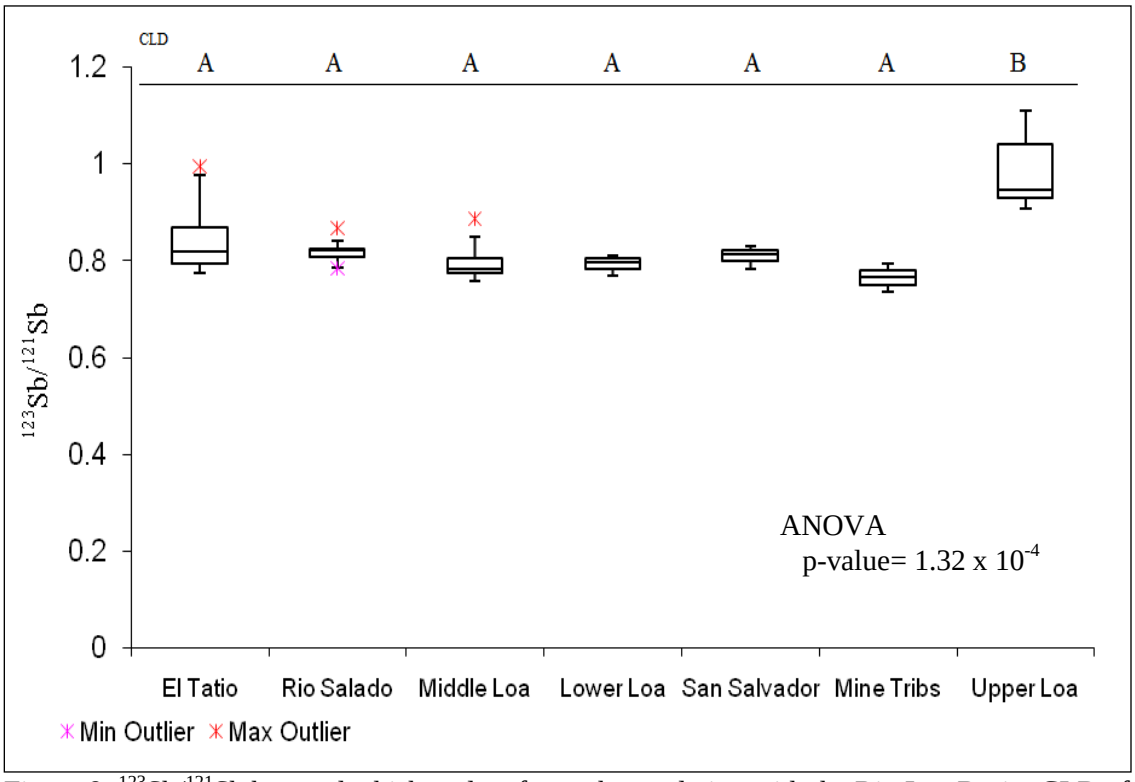

Figure 9: $^{123}Sb/^{121}Sb$ box and whisker plots for each population with the Rio Loa Basin. CLD of pairwise comparisons of means shows that the Upper Loa is statistically different from the other populations.

Labels	El Tatio	Rio Salado	Middle Loa	Lower Loa	San Salvador	Mine Tribs	Upper Loa
Min	0.774	0.784	0.757	0.768	0.784	0.735	0.907
Q_1	0.793	0.807	0.772	0.782	0.798	0.750	0.929
Median	0.819	0.819	0.782	0.797	0.812	0.765	0.945
Q_3	0.867	0.820	0.803	0.803	0.821	0.779	1.039
Max	0.996	0.867	0.887	0.810	0.831	0.794	1.110
IQR	0.073	0.013	0.031	0.021	0.023	0.030	0.110
Upper Outliers	1	1	2	0	0	0	0
Lower Outliers	0	1	0	0	0	0	0

Table 9: Statistical values for $^{123}Sb/^{121}Sb$ box and whisker plot

Lead Isotopic Analysis within the Rio Loa Basin

Box and whisker plots of lead isotopes were created using the ratios of $^{206}Pb/^{207}Pb$, $^{206}Pb/^{208}Pb$, and $^{207}Pb/^{208}Pb$ (Figure 10a-c). Overall, the analysis revealed that lead isotopic ratios between mine derived sediment, the El Tatio Geyser Field, and the background material (Upper Loa) were similar. Test results for a one way ANOVA using pairwise comparisons of means indicated that ^{206}Pb /^{207}Pb, $^{206}Pb/^{208}Pb$, and $^{207}Pb/^{208}Pb$ have p-values of 0.5949, 0.06615 and 0.113, respectively. All determined p-values were above the 0.05 threshold p-value at 95% confidence, therefore the null hypothesis could not be rejected. Because of this, the lead isotopes are assumed to be uniformly distributed throughout the Rio Loa Basin and are not utilized for tracer analysis.

Interestingly, t-tests between populations designated that El Tatio Geyser Field was statistically different than the Rio San Salvador for $^{206}Pb/^{208}Pb$, and $^{207}Pb/^{208}Pb$ ratios (Figure 10b,c) (Appendix A). For $^{206}Pb/^{208}Pb$, and $^{207}Pb/^{208}Pb$ the p-values for t-tests between El Tatio and the Rio San Salvador were determined to be 0.0367 and 0.0481, respectively (Appendix A). Because of this, the CLD indicates that El Tatio and the Rio San Salvador are separate populations from each other. However, El Tatio and the Rio San Salvador are not statistically different from all the other populations within the basin because CLD indicates an "AB" designation for all of the other populations within the basin (Figure 10 b,c). $^{206}Pb/^{208}Pb$ and $^{207}Pb/^{208}Pb$ may hold promise in future contaminant studies, but for this particular study the means were not statistically different and cannot provide contaminant tracer for the basin.

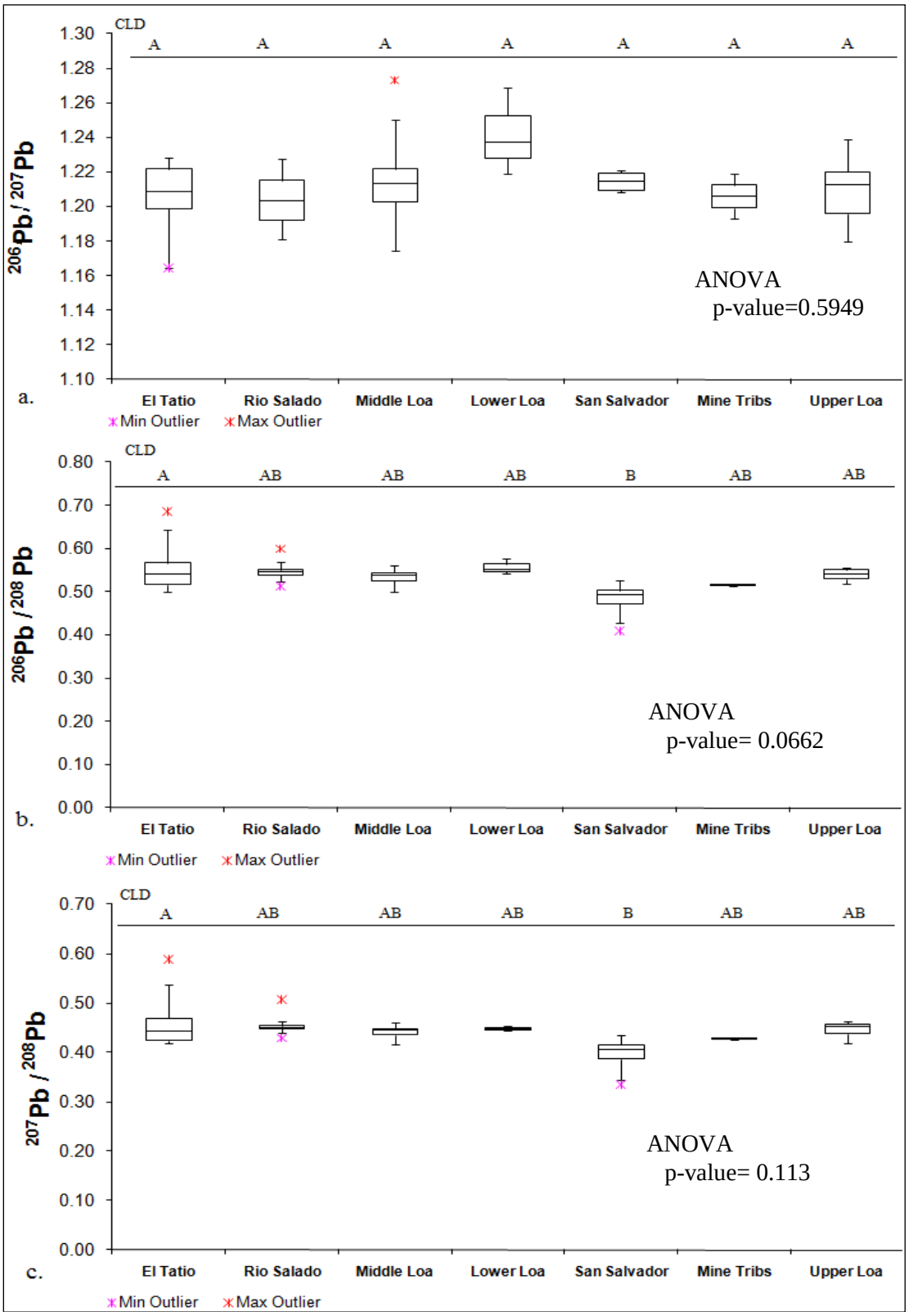

Figure 10: Analysis of lead isotopes. CLD indicates that all ratios of lead isotopes are above the 0.05 threshold p-value; therefore they are not statistically significant at this confidence level.

Spatial Changes in Geochemistry: Upper to Lower Loa Drainage System

Column plots showing downstream changes in total concentrations and ratios provided additional insights into contaminant input within a particular river reach. Reach-based analysis was done within the Upper to Lower Loa drainage system to detect specific input locations of arsenic, antimony, copper, and lead. This segment of the River extends from the headwaters of the Upper Rio Loa located near sample site UL-1, downstream through the Middle Loa and Calama Basin, and ultimately into the Lower Loa located after the confluence of the Rio San Salvador and the Rio Loa (Figure 11). For reach-based analysis, only surface samples (channel and floodplain deposits) were analyzed. Within the Upper Loa drainage system, concentrations of copper, antimony, and lead are generally larger within the floodplain deposits than within the channel bed deposits (Figure 12 b-d).

Total Arsenic Concentrations

Total concentrations of arsenic show almost the opposite trend, where concentrations are larger within the channel than nearby floodplain deposits for the RL-3 and RL-2 site (Figure 12a). Total arsenic concentrations within the Upper Loa drainage system are relatively low within the headwaters, exhibiting a notable increase in concentration within the floodplain sample at UL2-FF. After the confluence of the Rio Salado, concentrations increase from 50 ppm to 275 ppm within the RL3-C sample. Channel bed arsenic concentrations drop after the confluence of the Rio San Salvador (Figure 12a).

Total Copper Concentrations

Total copper concentration within the floodplain sample, UL2-FF, is an order of magnitude higher than both UL1-C and UL2-C, and 4 orders of magnitude higher than UL3-C (Figure 12b). All other concentrations within the samples collected downstream are much lower.

Within the Upper Loa drainage system, no elevated point source of copper contamination can be detected. Interestingly, no noticeable increase in copper concentrations occur downstream of the Rio San Salvador, which is known to drain metal contaminants from the Chuquicamata mine.

Total Antimony Concentrations and Antimony Isotopes

Within the headwaters of the Upper Loa drainage system, total antimony concentrations are below 11 ppm. Downstream of the confluence with the Rio Salado, antimony concentrations increase systematically until reaching sample RL3-a, located within the Middle Loa, after the confluence with the Rio San Salvador, no additional spikes in antimony concentration are present (Figure 12c).

In reference to the antimony isotopes, the Upper Loa samples (UL1, UL2, UL3, and UL4) and additionally, RL3- C, all contain isotopic signatures which are larger than the samples collected further downstream around the town of Calama, within the Middle Loa, and the Lower Loa downstream of the Rio San Salvador (i.e. Chuquicamata) (Figure 13d).

Total Lead Concentrations and Lead Isotopes

Similar to total copper concentrations, lead concentrations observed within the UL2-FF sample were nearly an order of magnitude higher than the other samples collected within the Upper Loa. No other notable increase in lead concentrations occurs along the Upper Loa drainage system. Concentrations within the floodplain deposits are higher than those seen within the channel bed deposits (Figure 11d). Lead isotopic ratios along the Upper Loa drainage system exhibit similar isotopic values (Figure 13a-c).

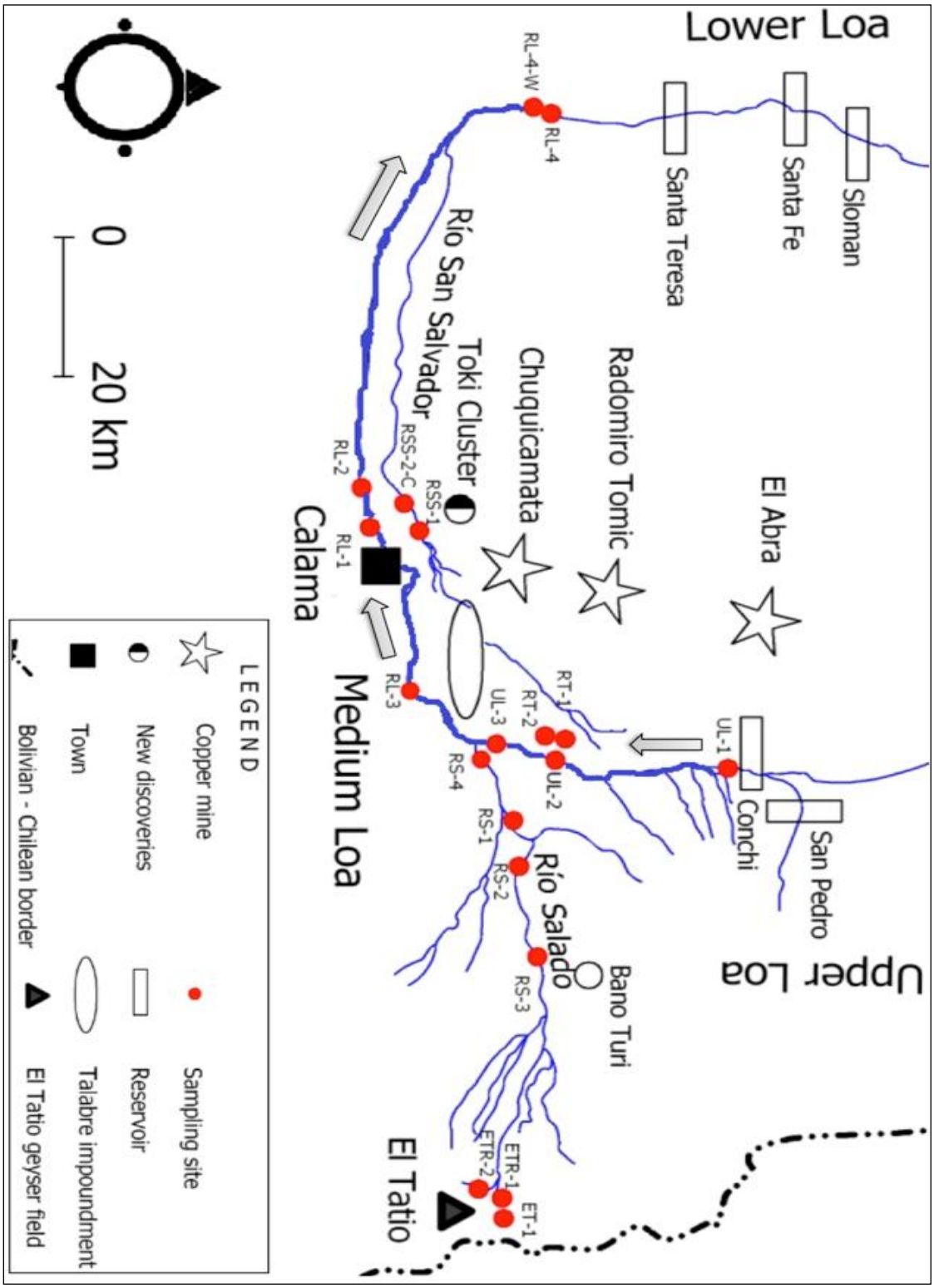

Figure 11: Location map of Upper to Lower Rio Loa Drainage System. Grey Arrows represent flow direction of analyzed reach.

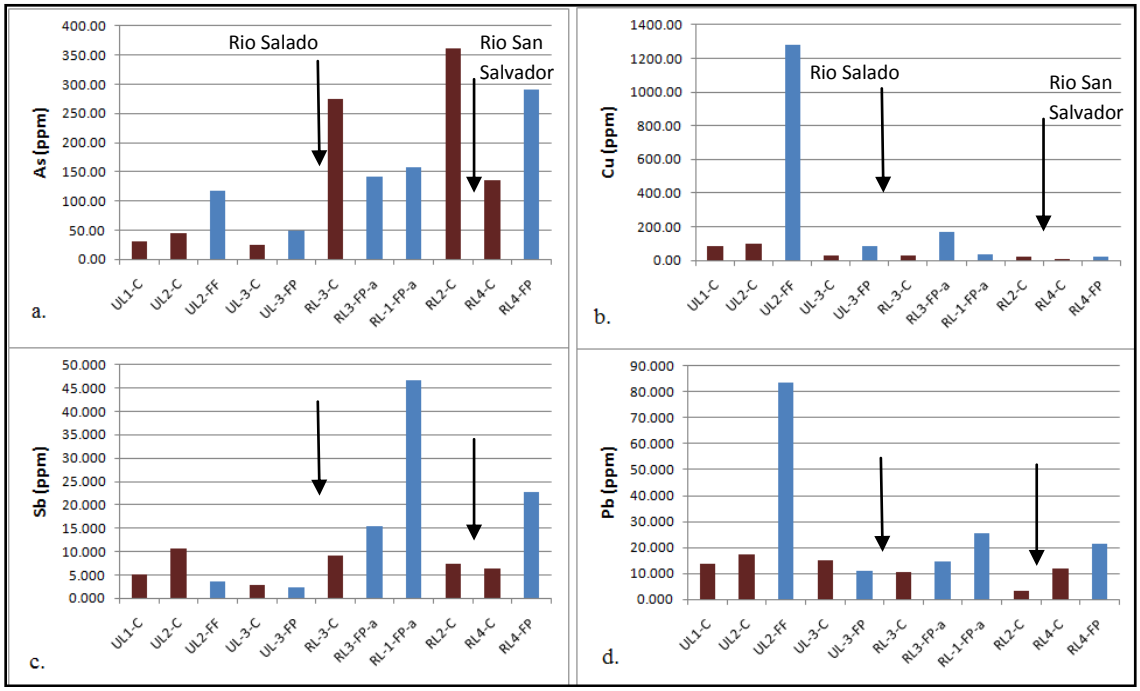

Figure 12a-d: Concentrations of arsenic, copper, antimony, and lead (ppm) within the Upper to Lower Rio Loa-Rio Loa drainage basin. Arrows represent input location of named tributary. Burgundy columns represent channel bed deposits whereas blue columns represent floodplain deposits.

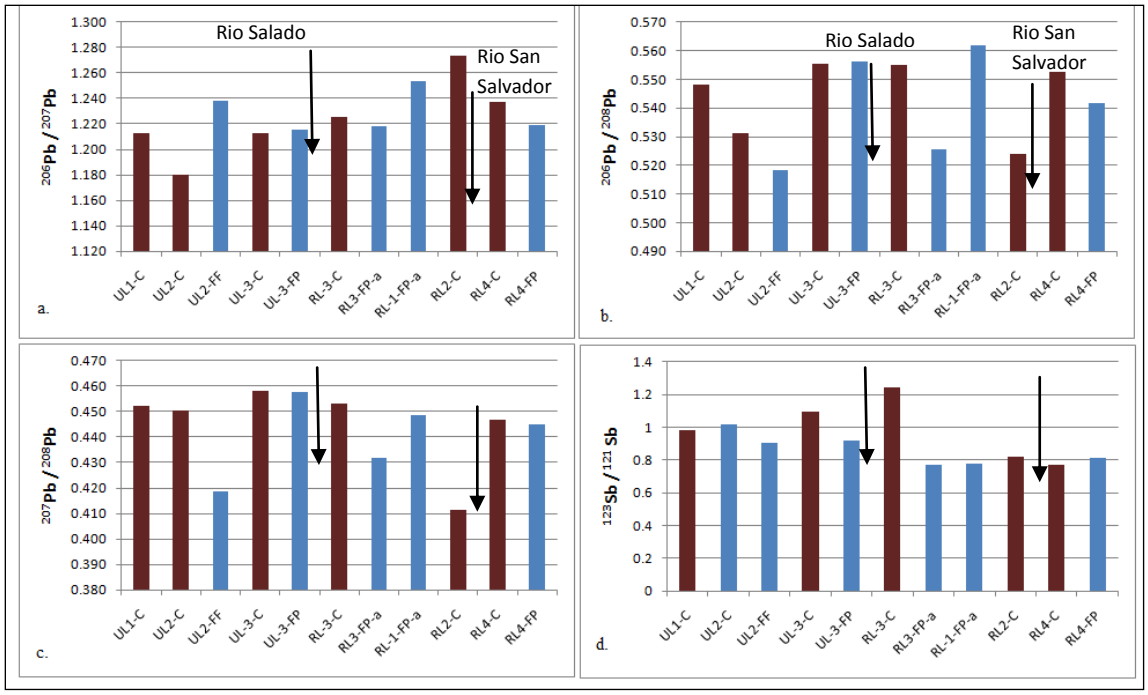

Figure 13a-d: Analysis of lead and antimony isotopes within the Upper to Lower Rio Loa drainage system. Arrows represent input location of named tributary. Burgundy columns represent channel bed deposits whereas blue columns represent floodplain deposits.

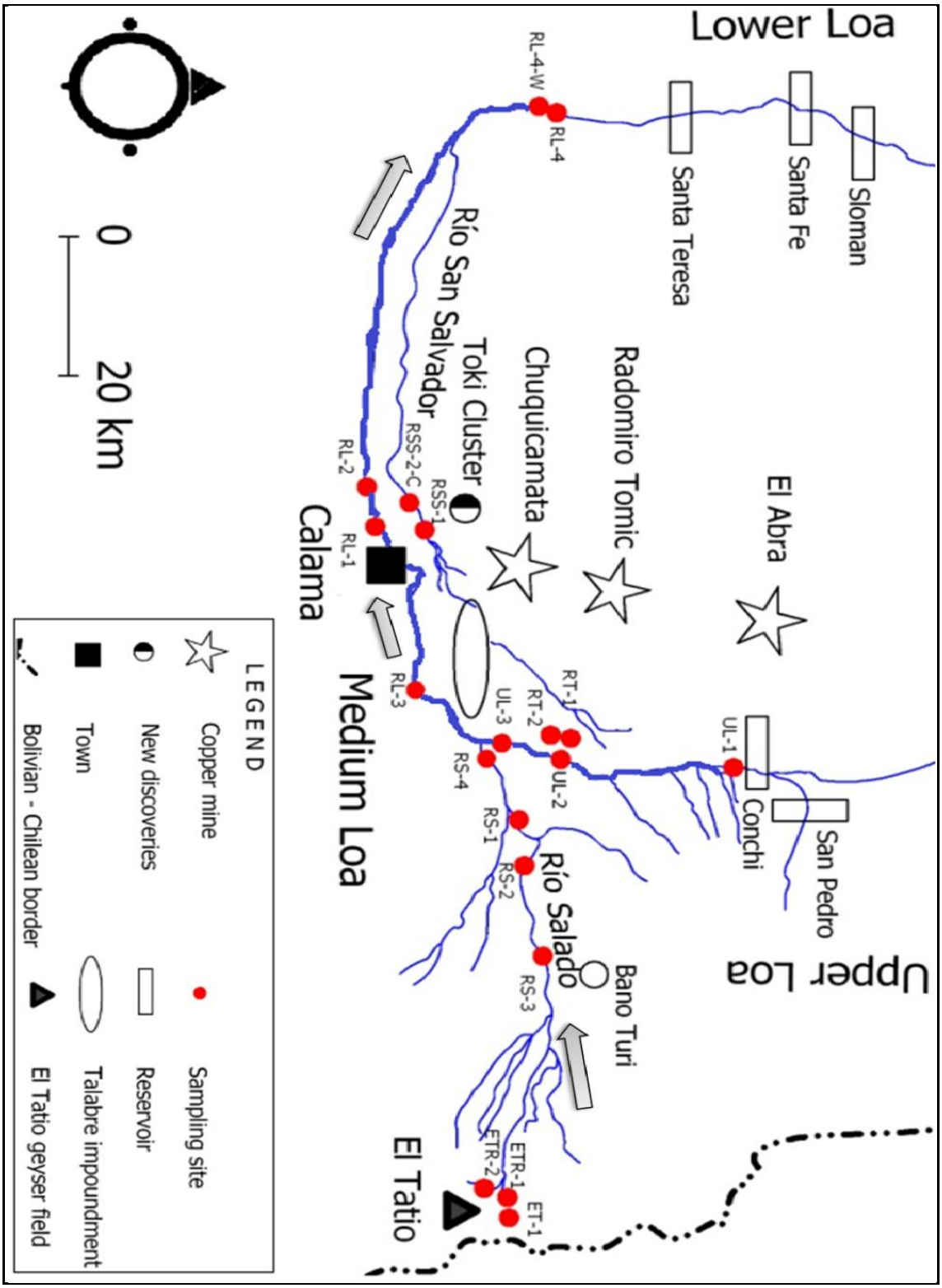

Figure 14: Location map of El Tatio-El Salado-Rio Loa Drainage System. Grey Arrows represent flow direction of analyzed reach.

Spatial Changes in Geochemistry: El Tatio-Rio Salado-Rio Loa Drainage System

The El Tatio-Rio Salado-Rio Loa drainage system begins downstream of the El Tatio Geyser Field within the channel of the Rio Salado at sample RS-3-C and extends downstream through the Rio Salado, into the Middle Loa and ultimately into the Lower Loa (Figure 14). Similar to the Upper Loa to Lower drainage system, a reach based analysis was performed using only surface samples within the channel bed and upper floodplain deposits. Column plots showing the downstream variations within the streambed sediments were produced for total concentrations of arsenic, copper, antimony, and lead, as well as for isotopes of lead and antimony (Figures 15 and 16).

Total Arsenic Concentrations

Reach-based analysis on the total concentrations of arsenic showed higher average concentrations from samples taken within the Rio Salado in comparison to samples located downstream within the Middle and Lower Loa (Figure 15a). Samples RS3-C , RS3-FP-a, and RS1-C are on average higher in concentration than those noticed downstream, especially after the confluence of the Rio Salado and Middle Loa after sample RL3-C. Additionally, a decrease in arsenic concentration is noticed after the confluence of the Rio Loa with the Rio San Salvador.

Total Copper Concentrations

Reach-based analysis on copper concentrations reveals minor changes in the total concentrations along the channel suggesting a more systematic pattern of copper deposition within the channel than within floodplain deposits (Figure 15b). Copper concentrations within the floodplain deposits change frequently within one population area and also between population areas. Overall, channel samples located within the Rio Salado are higher in concentration compared to those within the Middle Loa and Lower Loa. A steady drop in concentration can be observed downstream within the Middle Loa and Lower Loa after the Rio San Salvador confluence.

Total Antimony Concentrations and Antimony Isotopes

Reach-based analysis of the total concentration of antimony showed floodplain deposits had a higher concentration in comparison to channel bed deposits (Figure 15c). The reach-based analysis was broken up into analyzing the channel bed deposits and then the floodplain deposits since they each demonstrate different depositional patterns. Within the channel bed deposits, samples upstream of the Rio Salado/Rio Loa confluence show high concentrations of antimony, which is most likely coming from the El Tatio Geyser Field. However, downstream of the Rio Salado/Rio Loa confluence, channel bed sediments decrease in antimony concentrations to an average of about 7 ppm throughout the rest of the reach. In comparison, floodplain deposits do not decrease systematically in a downstream direction. Sample RL-1-FP-a, located within the Middle Loa, has an antimony concentration (ppm) which is almost 2 times greater than the average antimony concentrations determined for both the Middle Loa and Lower Loa floodplains. Additionally, antimony isotopic analysis revealed the $^{123}Sb/^{121}Sb$ ratio had no schematic trends for reach based analysis (Figure 16d).

Total Lead Concentrations and Lead Isotopes

Similar to Sb, reach-based analysis on the total concentration of lead (ppm) revealed that floodplain deposits contained a higher concentration of lead than channel bed deposits (Figure 15d). No systematic downstream patterns in lead concentrations occur along the El Tatio-Rio Salado-Rio Loa reach and no particular point source of lead was recognized. Additionally, the reach-based analysis of $^{206}Pb/^{208}Pb$ and $^{207}Pb/^{208}Pb$ isotopes contained a similar ratio throughout the reach. The $^{206}Pb/^{207}Pb$ isotopic ratio increased slightly within the Middle Loa within both the floodplain and channel deposits to a ratio of 1.27, but decreased after input from the Rio San Salvador to a ratio of about 1.23 (Figure 16a-c).

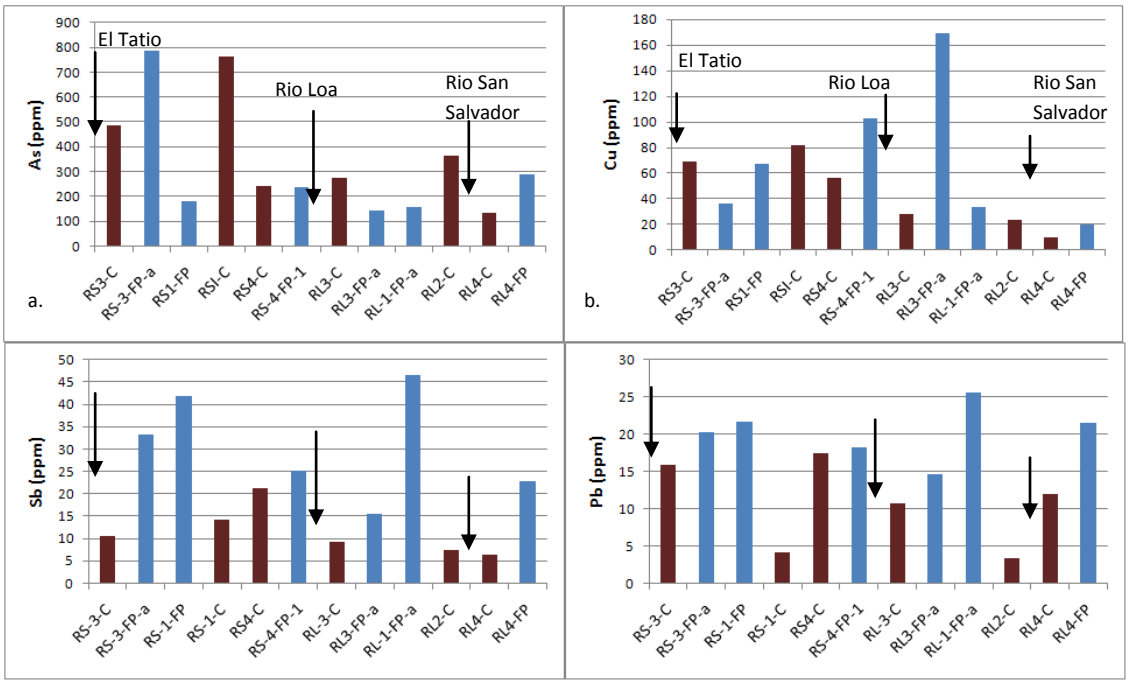

Figure 15a-d: Concentrations of arsenic, copper, antimony, and lead (ppm) Within the El Tatio-Rio Salado-Rio Loa drainage basin. Arrows represent input location of named tributary. Burgundy columns represent channel bed deposits whereas blue columns represent floodplain deposits.

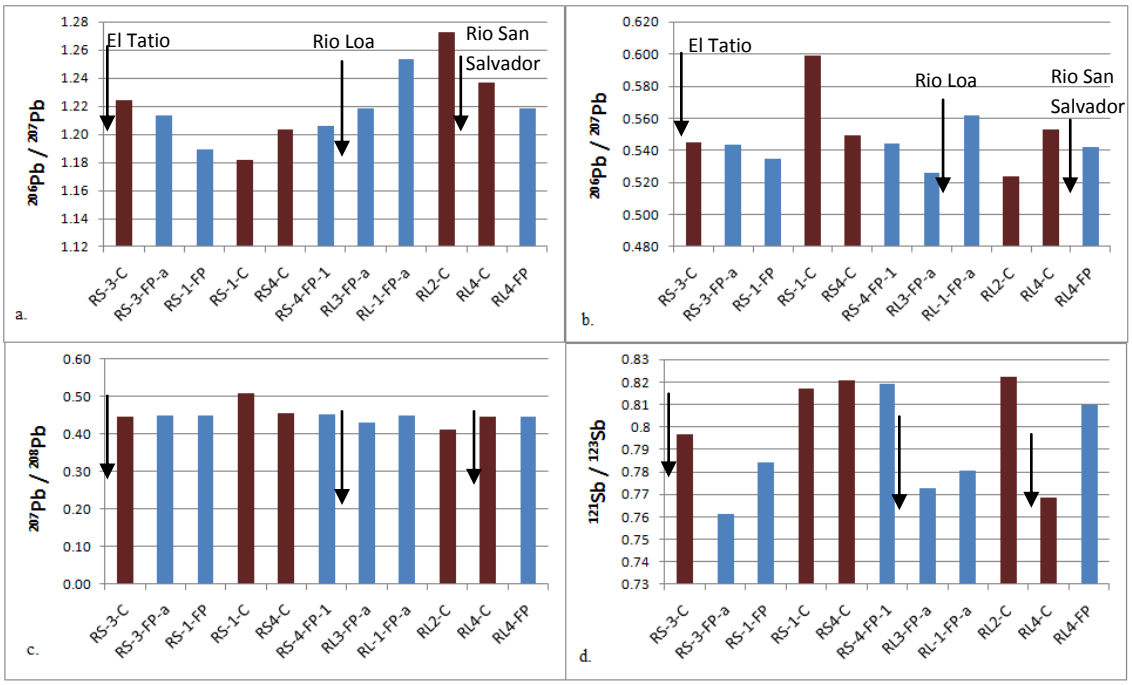

Figure 16a-d: Analysis of lead and antimony isotopes within the El Tatio-Rio Salado-Rio Loa drainage system. Arrows represent input location of named tributary. Burgundy columns represent channel bed deposits whereas blue columns represent floodplain deposits

Antimony/Copper Reach Based Analysis

Reach-based analysis was done on both the Upper to Lower Loa and the El Tatio-Rio Salado-Rio Loa drainage systems (Figure 17a-b). Within the Upper Loa, ratios of UL1-C and UL2-C are higher than ratios of UL2-FF and UL3-C indicating that copper concentrations within these samples are increasing. Interestingly, the sediments directly downstream of El Tatio have a relatively low ratio in comparison to sediments downstream within the Middle Loa, which is unexpected since El Tatio drains sediments containing high values of antimony. After the Rio Loa/Rio Salado confluence, the ratio within the Middle Loa and Lower Loa increases in a somewhat systematic pattern within both the floodplain and channel bed deposits. This indicates that either total copper concentrations are dropping, antimony concentrations are increasing, or both (Figure 17).

Floodplain Analysis

Floodplain deposits located at three locations along the Rio Salado and Middle Loa were analyzed at different depths below the surface for total concentrations of arsenic and antimony (Figure 18). Concentrations of arsenic range from around 80 ppm to almost 800 ppm. Antimony concentrations (ppm) are much lower, ranging from 10-33 ppm. There are some notable schematic downstream trends within the data. With respect to arsenic, concentrations are high within the Rio Salado (RS-3-FP-a and RS-3-FP-b), and decrease in average concentration within the floodplain sediment in the downstream direction. Additionally, the RL-3 floodplain site (located within the middle Rio Loa) shows a schematic decrease in arsenic concentration with depth (Figure 18). Concentrations of antimony within these three floodplain sites are similar within the Rio Salado. The RS-3 site has an average antimony concentration of 32 ppm, which

decreases with depth, but the RS-4 floodplain deposit contains an average concentration of 28 ppm, and increases with depth. Within the Middle Loa, lower values within the floodplains are observed with antimony concentrations between 12-17 ppm (Figure 18).

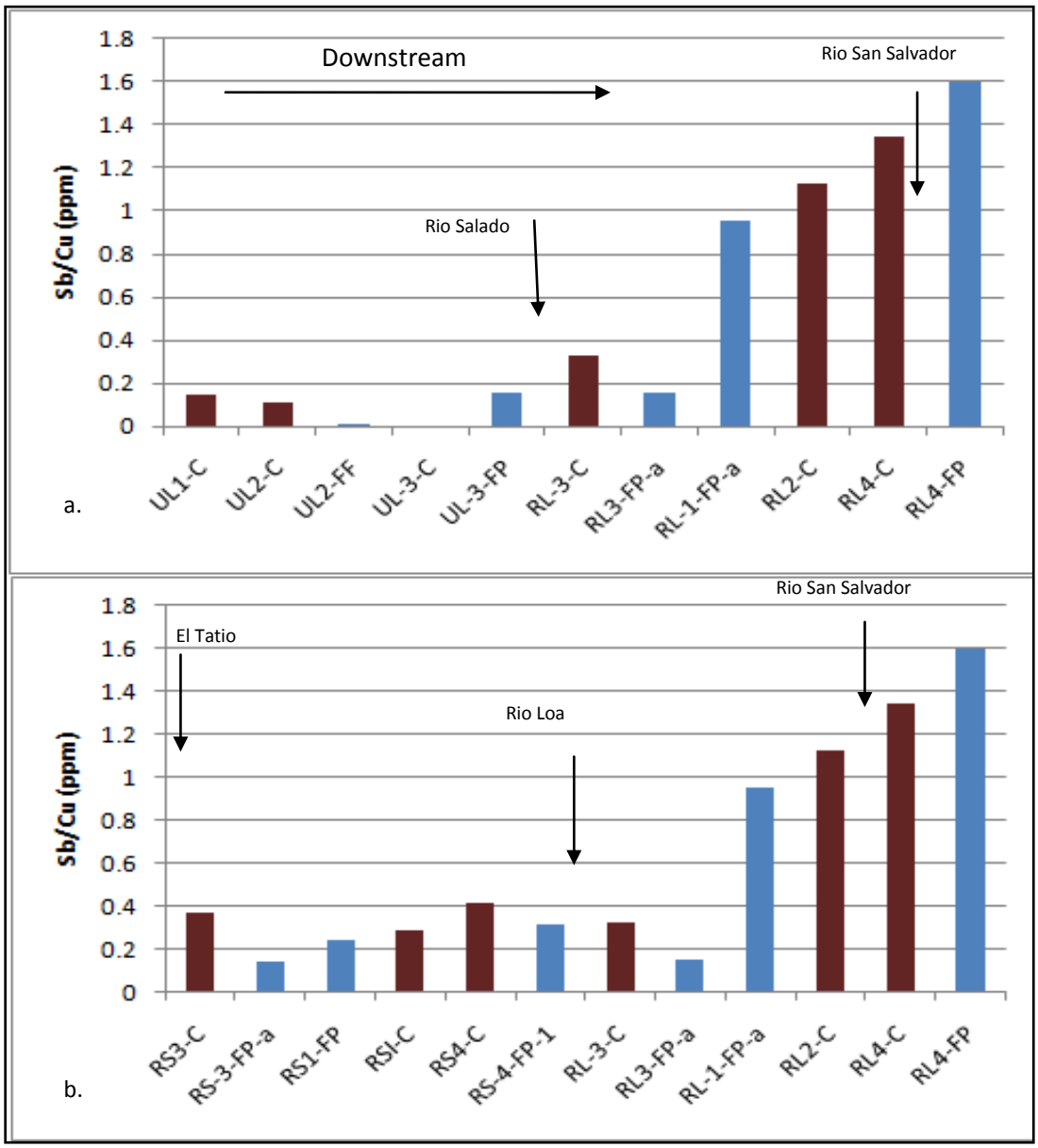

Figure 17a-b: antimony/copper ratios showing downstream variations within the Upper to Lower Loa drainage system (a) and the El Tatio-Rio Salado-Rio Loa drainage system (b). Black arrows represent the confluence of named fluvial system.

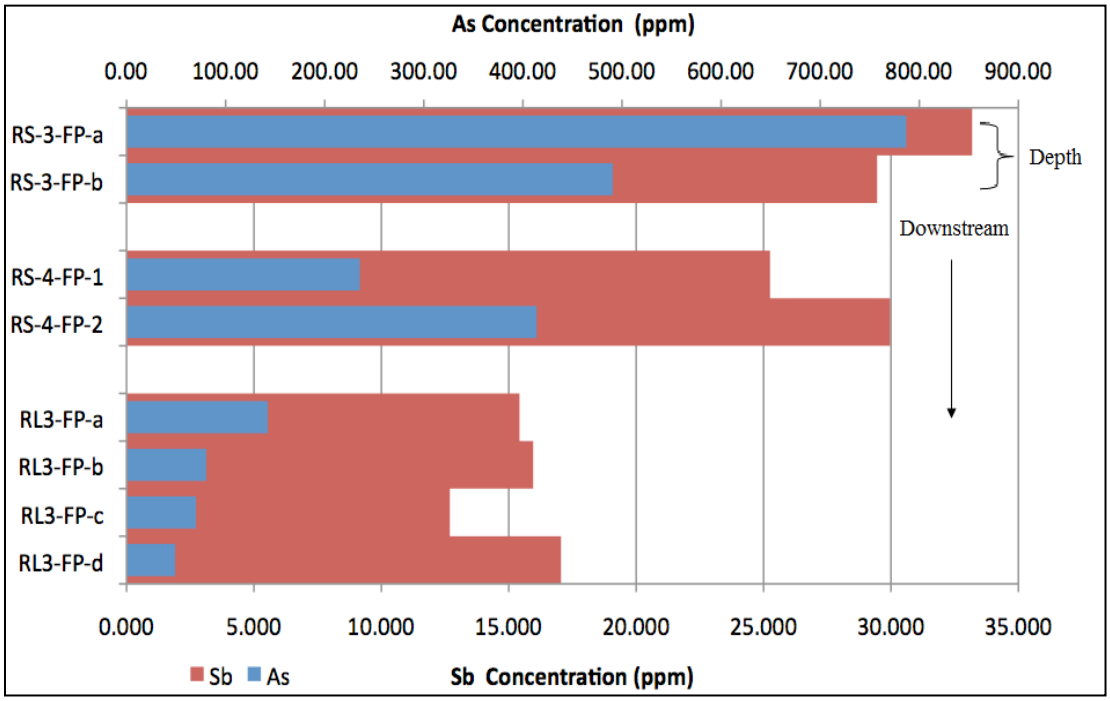

Figure 18: Depth Concentrations (arsenic and antimony) within three separate floodplain sites along Rio Loa and Rio Salado. See Figure 2 for sample site locations. Concentrations of arsenic (ppm) are plotted along the top axis while concentrations of antimony are plotted along the bottom axis.

Middle Loa Terrace Deposits

As mentioned, the RL-1 and RL-3 sampling sites were subdivided on the basis of their stratigraphic composition and then sampled for geochemical analysis. Within the RL-1 site, the channel sits in a wide valley composed of flat marshy terrain, which is used as pasture. The pasture is located 3.5-4 meters above the channel bed and the terrace shows lots of erosion features. Stratigraphic unit A is composed of silt-silt loam high in organic matter. Unit B is thin and composed of re-worked silt-sized ash deposited by the Rio Loa from a nearby volcano. Unit C is a silt-loam and rests on top of the eroded loamly-silt surface of unit D. Lastly, Unit D is a red soil surface, which contains carbonate and evaporate nodules.

The RL-3 terrace is spatially extensive and is composed of eight separate stratigraphic units. The surface of the terrace forms a highly eroded playa surface composed of red silt particles. The floodplain near the stream is well defined and is covered in dry species of grasses.

The channel is fast flowing and about 2.5 m deep with wetland grasses along the margins. Units A-F are all composed of silt-sized particles, that become more compact (harder) with depth. Unit G is composed of silt-sized particles near the top and becomes more organic with depth. Unit H is a paleo-soil composed of loam and fine sand-sized particles.

The antimony/copper ratio was used to quantify the dominant sediment contributor at the time the terrace was formed (Figures 19 and 20). Labels were put on the photographs to show how the stratigraphic units within the terraces were subdivided for sampling and analysis. Overall, the concentrations of arsenic are higher than the values for antimony in both terraces. The concentrations of arsenic range from 112-167 ppm within the RL-1 terrace (Figure 19), and between 330-1713 ppm within the RL-3 terrace site (Figure 20). Antimony concentrations within the RL-1 terrace range from 50-110 ppm, while the RL-3 terrace ranges from 15-50 ppm. Total arsenic concentrations are similar overall for the RL-1 terrace, however within the RL-3 terrace, noticeable increases in arsenic occurs within stratigraphic unit E and F (Figure 20). The most distinct pattern seen in both terrace sites is the increase in antimony concentrations with depth. This increase is seen within stratigraphic units D of the RL-1 terrace site (Figure 19), and unit E within the RL-3 terrace (Figure 20).

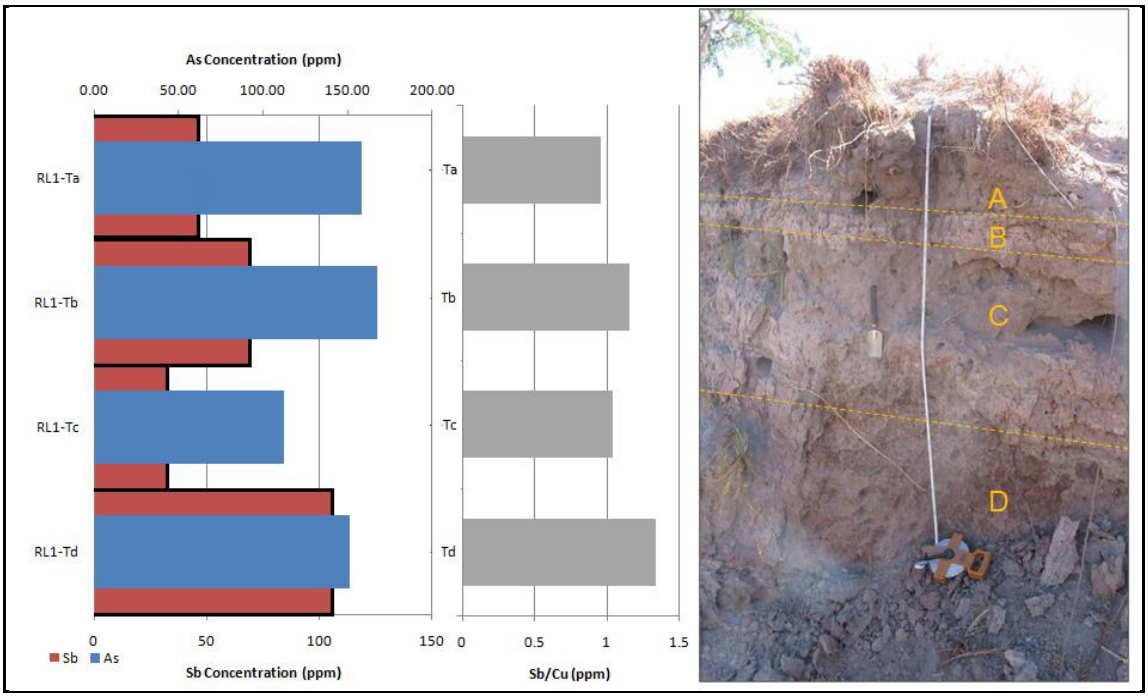

Figure 19: Variations in arsenic and antimony concentrations (ppm) with depth in terrace deposits described and sampled at RL-1 within the Calama basin. Photograph on Right shows samples stratigraphic units

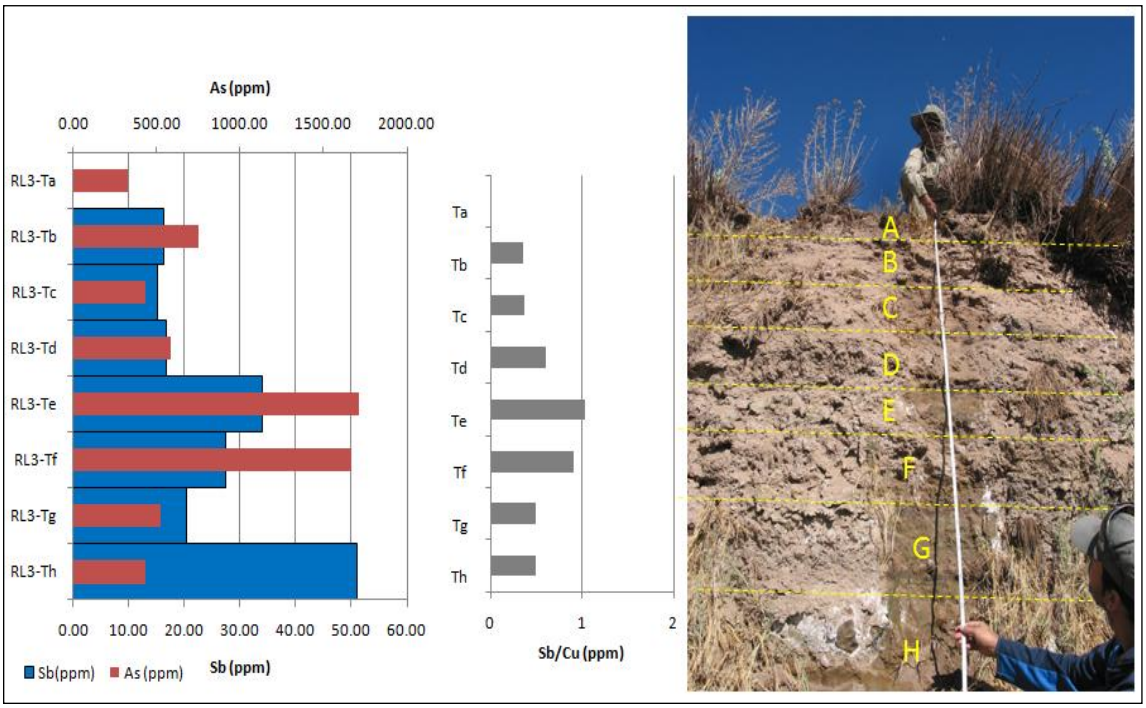

Figure 20: Depth Concentrations (arsenic, antimony) and antimony/copper ratios within RL-3 terrace site along the Rio Loa.

Sequential Extraction Analyses

Sequential extraction analyses revealed that arsenic has a high mobility within the basin because it binds to multiple substrates within the river column and it may transfer to different particle types within the water as the river transports sediment downstream (Figure 21a). An assumption in the use of chemical tracers for sediment bound contaminants is that they are conservative, meaning they move with the sediment without entering the aqueous phase. At El Tatio, arsenic is mostly associated with the carbonate fraction, with the exchangeable ion fraction having the second largest percentage. However, within the Rio Salado, the Fe-Mn oxides and carbonates exhibit similar percentages of arsenic, whereas the exchangeable arsenic decreases dramatically downstream of El Tatio.

The Upper Loa was determined to have a lower amount of arsenic within the residual fraction than the Rio Salado (Figure 21a). Downstream, the Middle Loa displays an interesting increase in both the Fe-Mn oxide and carbonate fractions while the percentage of arsenic associated with the exchangeable, organic, and residual fractions decreased within this section of the river. The Middle Loa also has the lowest amount of arsenic within the residual phase, indicating mobility within this section is high because it is predominately bound to particles where it can be easily desorbed. Downstream of the Chuquicamata mine, the arsenic found within the Fe-Mn oxide fraction is slightly higher, while the exchangeable and organic fractions are slightly lower relative to the dominant arsenic absorbing substrates within the Rio Salado and the Middle Loa.

Copper is predominately attached to Fe-Mn oxides or organic matter within the water column in all sample populations (Figure 21b). Only about 5-10 percent of the copper was found adsorbed to the carbonate particle surfaces and an even smaller percentage was found within the exchangeable fraction. The residual fraction extraction suggests some of the copper, less than 35 percent, is being absorbed within the crystalline structure of the particles. Within each population

the percentage of copper, which changes substrates it is attached to, is low. For this reason, copper is not considered to be mobile because the predominate substrate it is adsorbed to is not changing between sample populations.

The sequential extraction on antimony revealed that it is tightly bound within the residual phase and therefore its mobility within the water column, and potential for biological uptake, is limited (Figure 21c). The most noticeable deviation is from samples taken downstream of Chuquicamata, in which some antimony is associated with the exchangeable, carbonate, Fe-Mn oxide, and organic fractions. Although the amount of mobile antimony coming from Chuquicamata is lower than 25 percent, the other 75 percent is bound within the residual phase. El Tatio Geyser Field contains the highest amount of antimony found within the residual phase. This is possibly because antimony from the geyser basin is being precipitated from extremely hot emergent waters and as the water cools, the antimony absorbs with silica, forming an opal amorphous mineral (Landrum et al., 2009).

Lead was also found tightly bound to sediment since the largest percentage of lead was found within the residual phase (Figure 21d). Lead is commonly seen tightly bound with sulfur to create sulfide minerals such as galena, which have been known to form in hydrothermal areas (Landrum et al, 2009). Only about 10-20 percent of the time, lead was found within the organic fraction (Figure 21d). The Upper Loa, located upstream from the drainage from El Tatio, contains the highest percentage of lead adsorbed to particles (i.e., not found within the residual fraction). This loosely bound form of lead is also present within the Middle Loa in minor amounts, but is diluted by lead in the residual fraction coming from the El Tatio Geyser Field.

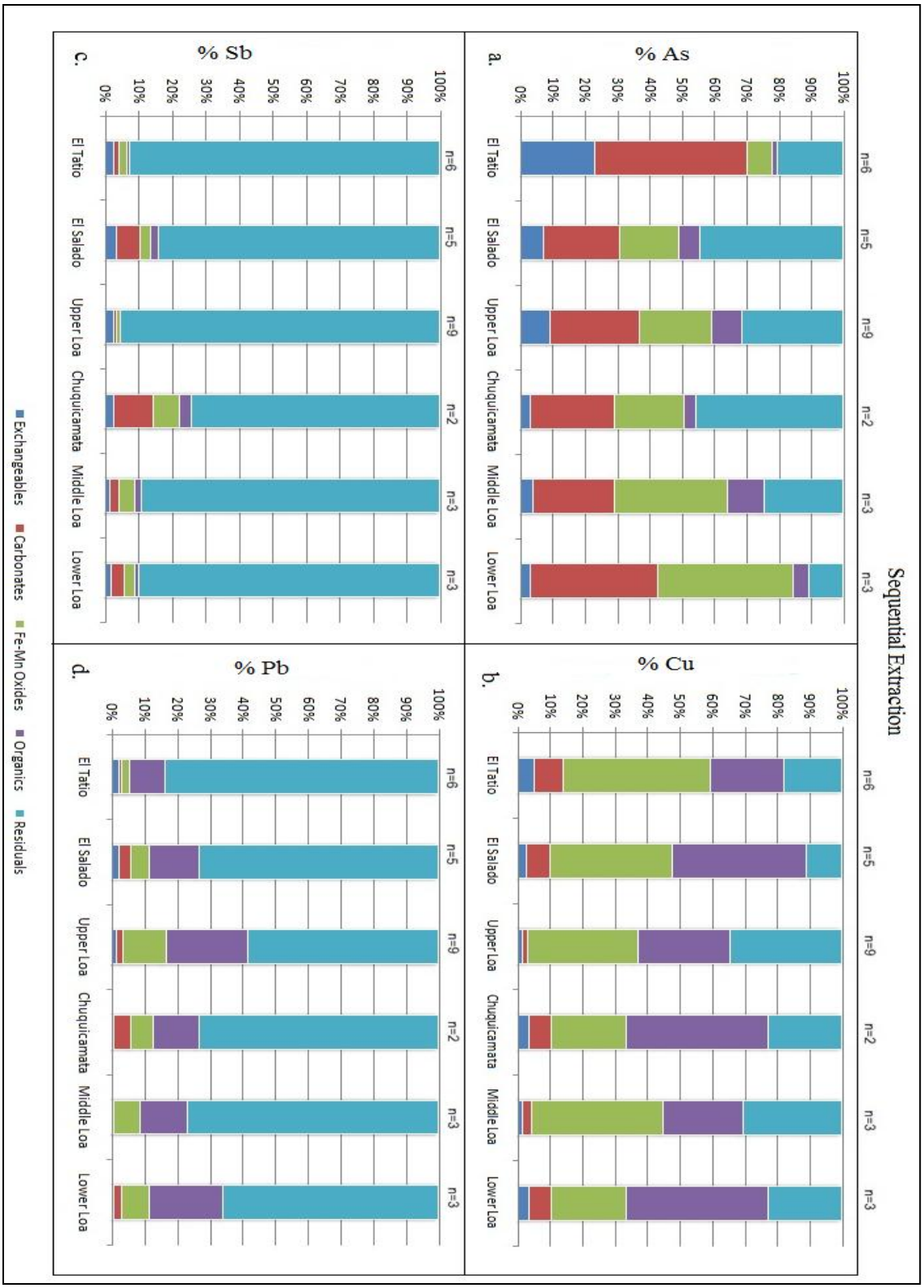

Figure 21a-d: Analysis of Sequential Extraction; arsenic is bound within multiple extractions, while lead and antimony are primarily found in the residual phase. Copper was determined to be mostly within the Fe-Mn oxide and organic matter fractions.

CHAPTER FIVE: DISCUSSION

Several sources of toxic trace metals exist within the Rio Loa Basin, of which El Tatio and mining operations are the two largest contributors. During this investigation, several different methods to determine the influx of trace metals to the river from each of the potential sources were utilized. These methods include (1) spatial trends in elemental concentrations, (2) elemental ratios, and (3) lead and antimony isotopes. The usefulness of the various methods will be discussed in the following paragraphs, starting by examining spatial trends in arsenic, antimony, copper, and lead concentrations along the drainage network.

Total Elemental Concentrations

Total Arsenic and Antimony Concentrations

The semi-systematic downstream decreases in arsenic and antimony concentrations within the deposits of the Rio Loa Basin indicate that El Tatio Geyser Field is the largest source of these toxic metals (Figures 5 and 6). Mining operations also appear to contribute a lesser amount of arsenic and antimony to the river, and therefore add to the contaminant load. For example, within the Upper Loa, a small contribution of arsenic and antimony from mining operations at El Abra and Radiomiro Tomic is suggested by a minor increase in concentration, especially after sample UL2-FF (Figure 12a,c). Further downstream, dilution and/or the deposition of contaminated particles slowly decreases the arsenic and antimony concentrations along the channel until the Rio Salado confluence, where arsenic and antimony concentrations increase dramatically. This dramatic increase in concentration predominately results from the influx of sediment transported from the El Tatio via the Rio Salado. As shown in figure 15a and c, after antimony and arsenic enters the Middle Loa from the Rio Salado, it is quickly diluted through mixing of predominantly clean sediment from the Upper Loa. This trend is seen through the decrease in concentrations in the downstream direction throughout the Middle Loa. After the

confluence of the Rio San Salvador, arsenic and antimony concentrations decrease rapidly again, presumably due to dilution as sediment characterized by low arsenic and antimony concentrations enter the Rio Loa from the Rio San Salvador and mixes with the contaminated sediment within the lower Loa.

Within the Middle Loa, the increase in concentrations of antimony in the floodplains and the increase of arsenic in the channel bed sediment is most likely related to (1) grain size differences common in the channel bed and floodplain deposits, and (2) partitioning differences of the two elements (Figures 12 and 15a,c). The sequential extraction data indicates that antimony is primarily associated with the residual phase. This is consistent with earlier studies (e.g. Landrum et al., 2007) that have argued that antimony is contained within the structure of silica minerals precipitated from hot solutions at El Tatio, making it immobile within the river system.

Two separate dispersal pathways could lead to high concentrations of antimony within the floodplain deposits of the Middle and Lower Loa. First, contaminated sediment coming from El Tatio are deposited within the Middle Loa. Hydraulic sorting of the particles will deposit particles on the floodplain of the Rio Loa during normal conditions. During a flood event, the floodplains are inundated and the more mobile elements will be picked up by the floodwater and transported downstream, while the non-mobile elements will stay within the floodplain. Arsenic is considered much more mobile than antimony, so during a flood event, arsenic may be dissolved within the floodwater and flushed out of the floodplain deposits.

The second pathway leading to an increase of antimony within the floodplain sediment is the erosion of older terrace deposits. During the latest El Nino/La Nina flood event in 2001, older terraces were inundated and eroded by floodwater. The eroded sediments were re-worked into the floodplain deposits of the Middle Loa. Flood deposits after the event were observed to be almost a meter thick in some locations within the Calama Basin (Houston, 2006). Both arsenic and

antimony were found to be above background values within the terraces analyzed at two sites (Figures 19 and 20). However, since arsenic is the more mobile element of the two, it is less likely to be deposited with sediment on the floodplain and more likely to be dissolved within the water column and transported downstream. Antimony presumably remains with the sediment on the floodplain after the flood. For this reason, a higher concentration of antimony, in comparison to arsenic, will be observed within the floodplain deposits of the Middle and Lower Loa.

Total Copper Concentrations

Analysis of total copper concentrations found that mining operations contribute a large amount of copper into the Rio Loa Basin (Figure 7). The Rio San Salvador, which drains the Chuquicamata mine, and the two smaller mines (El Abra and Radiomiro Tomic) exhibit high concentrations of copper (Figure 7). The low concentrations of copper observed in samples from El Tatio and along the Rio Salado suggest that there was very little copper coming from these two sources. The lowest concentrations of copper are found within samples taken from within the Upper Loa supporting the argument that these sediments reflect the background values of copper for the basin as a whole.

Interestingly, reach-based analysis revealed that the Lower Loa had the lowest median concentration of copper even though this reach is located directly downstream of the Rio San Salvador, which exhibited very high concentrations of copper. The sequential extraction results of copper showed it was mostly present within the Fe-Mn oxide and organic matter fractions (Figure 21b). Copper released from Chuquicamata via the Rio San Salvador, will be quickly adsorbed to any free surface area of Fe-Mn oxides and/or organic matter substrates which are present within the channel bed and will not be transported long distances downstream in solution. The most probable situation is that a majority of the copper released has already been adsorbed to Fe-Mn oxides and/or organic matter within the Rio San Salvador before it could be transported to the

Lower Loa due to sediment storage and dilution from clean sediment within the Rio San Salvador. Because of this, copper concentrations observed within the Lower Loa are not as high as to be expected.

Total Lead Concentrations

Schematic patterns for total lead input analysis proved difficult because the mean concentration for all the samples analyzed was similar (Figure 13a-b). That is, no schematic patterns exist, possibly because there is no point source of lead contamination other than the mineralized rocks that underlie the basin as a whole. They are weathered and eroded at similar rates throughout the entire Rio Loa Basin, resulting in similar lead concentrations within the alluvial sediments.

Use of the Antimony/Copper Ratio as a Geochemical Tracer

A box and whisker plot of the antimony to copper ratio suggests that it may serve as a simple parameter to distinguish anthropogenic and natural sources of contaminated sediment in the Rio Loa (Figure 8). Since the mining operations of Chuquicamata and El Abra and Radiomiro Tomic have high concentrations of copper, they plotted low on the box and whisker plot. Population areas high in antimony and low in copper, such as the El Tatio Geyser Field, plotted very low on the box and whisker plot. The mixing of sediment from the El Tatio Geyser Field and mining contaminated sediment from the Upper Loa is noticeable on the plots by the large IQR observed within the Middle Loa, and to a lesser extent, the Lower Loa (Figure 8). The Rio Salado is observed to have a much lower antimony/copper ratio in the El Tatio Geyser Field, possibly because of dilution factors which greatly influence the concentration of antimony within this reach. Additionally, a small input of copper into the Rio Salado could be via small copper mining operations which are present within the foothills of the Andes Mountains.

The antimony/copper ratio increases downstream within the Rio Salado-Rio Loa-Lower Loa system (Figure 17b). This is due to the total copper concentration within Rio Loa decreasing downstream, while the antimony concentration within the floodplains are either increasing or staying constant. The copper concentration within the Middle Loa and Lower Loa is decreasing for two separate reasons. First, sediment low in copper will be incorporated into the channel, diluting the overall concentration of copper within the Rio Loa as it flows downstream. Additionally, the partitioning of copper onto particles of Fe-Mn oxides and/or organic matter within the channel bed limits the transport of copper downstream. This is especially true if the copper enriched particles are deposited on a floodplain, as is demonstrated by the high concentrations of copper within sample RL3-FP-a (Figure 15b).

The observed increase in antimony within the Middle Loa may be due to the erosion of older terrace deposits and the subsequent reworking of these particles into the floodplain and channel bed deposits. Older terrace deposits sampled at RL-3 and RL-4 presumably consisted of contaminated sediment derived mostly from the El Tatio Geyser Field because they contained high concentrations of antimony and arsenic (Figures 19 and 20). The terraces contained low concentrations of copper, demonstrating that mining operations had little impact on the sediment in the Rio Loa at the time these terrace deposits were created. As these terraces are eroded, the antimony and arsenic contaminated sediment is transported downstream and deposited within both the channel bed and floodplain deposits of the Middle Loa and Lower Loa. Concentrations of arsenic are likely to be lower because during floods the floodplains are inundated and arsenic is leached from the sediments. Antimony does not dissolve out of the floodplain deposits since it is tightly bound within the crystalline structure of the sediment. Over time, the concentrations of antimony within the floodplain deposits will probably increase as the terrace sediments are eroded and re-worked into the floodplain deposits.

Isotopic Analysis

Improvements on instruments such as the Inductively-Coupled Plasma Mass Spectrometer (ICP-MS) and the Thermal Ionization Mass Spectrometer (TIMS) help expand upon the use of isotopes as contaminant tracers in environmental studies. Due to the complications of using total concentration data alone, isotopic tracers have given researchers the ability to more accurately trace contaminant sources and nutrient cycling in more detail and with better precision. Isotopic tracer methods have only recently been applied to the study of hydrophobic (sediment borne) trace metal contaminant flow pathways, and the field is rapidly growing with new advances in technology and instrument precision. Historically, isotopic tracers have been used in a wide range of hydrology studies where they are used to (1) determine the sources of water and solutes; (2) characterize water and contaminant flow paths and; (3) assess the biogeochemical cycling of nutrients (Miller and Orbock Miller, 2007). An isotope of an atom can either be stable or radioactive, and this depends on whether or not the isotope is decaying into other isotopes, by giving off different types of radiation.

In this study, stable isotopes of antimony and radiogenic isotopes of lead were analyzed for source determination. These isotopes were chosen because (1) lead isotopes are commonly used in environmental isotopic studies because they typically exhibit high fractionation ratios in most rock types and have been proven useful in tracer analysis; (2) antimony isotopes have proven to be useful in some environmental applications (Rouzel et al., 2003); (3) antimony concentrations within the Rio Loa Basin are high in comparison to average soil concentrations measured throughout the world (Miller and Orbock Miller, 2007); and (4) high concentrations of both lead and antimony within the residual fraction makes them promising in tracer analysis because they are moving with contaminated sediment instead of partitioning to various substrates and dissolving into the water column.

Antimony Isotopic Analysis

Antimony isotopes have not been extensively used as an environmental tracer, nevertheless, antimony isotopes show promise because the large range of isotopic values is dependent on the reduction and oxidation reactions which aid in the fractionation of antimony (III) and antimony (V) chemical species. Redox driven isotope fractionation, especially in hydrothermal areas, is known to naturally produce large fractionation values between oxidized and reduced species of antimony (O. Rouxel et al., 2003). As seen within the samples taken from the El Tatio Geyser Field, the antimony isotopic range of these samples is greater than all other locations within the basin (Table 9). The Rio Salado, Chuquicamata, and Lower Loa all contain smaller isotopic ranges in comparison. The mean isotopic value for the Upper Loa represents a much higher signature than the other populations (Figure 9). This likely results because the reach is not affected by antimony input from El Tatio; therefore the samples represent background isotopic ratios. Utilization of this method in studies with only one source of contamination could provide useful in determining hydrothermically contaminated material from background materials. However, in this particular study it provided little information in determining sources of contamination because the two sources being distinguished (i.e. mining operations and El Tatio) had similar ratios.

Lead Isotopic Analysis

Lead isotopes often provide an extremely useful tool in environmental studies for contaminant tracer applications. However, in the case of the Rio Loa basin, the mean isotopic signatures for all source populations are similar. Thus, lead isotopes cannot be used to distinguish between the contaminated sediment sources. One exception may be the identification of sediment from Chuquicamata using the $^{207}Pb/^{208}Pb$ ratio (Figure 10b). The mean signature is slightly lower for Chuquicamata compared to all the other sources within the basin, however additional samples (and sample analysis) are required to verify the potential trend. If Chuquicamata does in fact

have a different isotopic signature than the other sources, it would be an extremely useful tool in finding out how much contaminated sediment is coming from this mine.

Floodplains and Terraces

Floodplain deposits typically have high concentrations of contaminants due to hydraulic sorting between the larger and smaller particles. Smaller grain sizes within the floodplains may contribute to the larger concentrations being found within the floodplain deposits. Analysis of the terrace deposits at RL-1 and RL-3 provided an interesting history of changes in contaminant sources and pathways over time in the Rio Loa Basin (Figures 19 and 20). In the RL-1 terrace, section B is lighter in color and contains larger grain sizes, but is higher in both arsenic and antimony concentrations relative to section A and C within the terrace (Figure 19). These units were deposited possibly during a volcanic eruption, where the ash was transported by the river system and deposited on the floodplain.

The most interesting pattern observed within these two terrace sites is the noticeable increase in antimony concentrations with depth, observed within stratigraphic section E of RL-3 (Figure 19) and D of RL-1 (Figure 20). This suggests either (1) changes in mining procedures have decreased the input of antimony into the fluvial system, or (2) post-mining operations have diluted the antimony coming from El Tatio within the system. It is suspected that the surface of the terrace deposit must be from post-mining operations since previous literature suggests that during the latest El Nino/La Nina event in 2001, the Middle Loa terraces were substantially flooded, and deposits of a meter thick were reported in some areas (Houston et al., 2006). No simple method is available to date these two terrace deposits, but some evidence, like higher concentrations of antimony within the older deposits, suggests that El Tatio may have contributed more antimony into the Rio Loa in earlier times than it does today.

CHAPTER SIX: CONCLUSIONS

El Tatio Geyser Field contained very high concentrations of antimony, and mining operations contained the highest concentrations of copper relative to other source populations within the Rio Loa basin. Thus, the antimony/copper ratio proved to be the best method to distinguish source(s) of sediment contamination within the Rio Loa Basin. Moreover, antimony/copper data showed where contaminants, which were either contaminated from El Tatio Geyser Field or mining operations, were deposited. The Middle and Lower Loa were contaminated by both mining operations and El Tatio, but downstream the input from El Tatio was greater than that which was coming from the mining operations. A look at the older terrace deposits revealed that El Tatio Geyser Field was the main contributor of antimony (and sediment) at the time these deposits were created. Over time, large amounts of antimony have been built up within the layers of the terraces. As these terraces are eroded, the re-worked sediments are incorporated into the floodplains and to a lesser extent, the channel bed.

Copper concentrations decrease within the Rio Loa because of dilution and storage of sediment, most of which consists of Fe-Mn Oxides and/or organic matter. Since copper was determined to have a high affinity for Fe-Mn Oxides and organic matter, it is presumed that any copper released from both Chuquicamata and mining operations will absorb to these particles and will not be transported long distances downstream of the mining operation in solution. Additionally, these Fe-Mn and organic matter particles are deposited and diluted within the Rio San Salvador and not readily transported with the suspended or particulate load downstream. Thus, the low concentration of copper found within the Lower Loa after the confluence of the Rio San Salvador is explained by this process.

Isotopes of antimony and lead did not provide enough information to accurately distinguish between the anthropogenic (mining operations) and natural (El Tatio) sources of

contamination studied in this investigation. Lead was determined to be uniformly distributed within the entire basin of the Rio Loa due to similar bedrock throughout; therefore it was not helpful for this particular study. Antimony isotopes were able to distinguish background ratios from material which has been affected by contaminant input from El Tatio, but they were not able to distinguish between sediment from mining operations and El Tatio. Antimony isotopes may prove useful in similar studies which are attempting to quantify contaminated sediment from one source of hydrothermal contamination.

The objective of this study was to determine the degree of contamination within the Rio Loa Basin and distinguish the potential source(s) of contamination via the use of total concentrations of arsenic, antimony, copper, and lead and the ratios of antimony and lead Isotopes. A sequential extraction procedure on thirty of the samples within the basin aided in the analysis by determining how the selected elements are bound to the analyzed sediment, therefore providing geochemical data describing the most likely dispersal pathway, and mobility, of each element. Additionally, findings within the floodplains and terraces located within the Rio Loa Basin helped in interpreting a historical record of contamination within the basin, along with where additional contaminant input is occurring today.

WORKS CITED

Collins, A. L., and D. E. Walling. Selecting Fingerprint Properties for Discriminating Potential Suspended Sediment Sources in River Basins. *Journal of Hydrology*. **2001**. 261.218-44. Elsevier.

Baker, Victor R. Stream-channel Response to Floods, with Examples from Central Texas. *Geological Society of America Bulletin* 88.8. **1977**.1057.

Buonicore, Anthony J. Cleanup Criteria for Contaminated Soil and Groundwater. West Conshohocken, PA: ASTM, **1996**.

Garcia-Valles, M., J. L. Fernandez-Turiel, D. Gimeno-Torrente, J. Saavedra-Alonso, and S. Martinez-Manent. Mineralogical Characterization of Silica Sinters from the El Tatio Geothermal Field, Chile. *American Mineralogist*. **2008**. 93.1373-383.

Houston, John. Variability of Precipitation in the Atacama Desert: Its Causes and Hydrological Impact. *International Journal of Climatology* . **2006**. 26.15.2181-198.

Landrum, J. T., P. C. Bennett, A. S. Engel, M. A. Alsina, P. A. Pasten, and K. Milliken. Partitioning Geochemistry of Arsenic and Antimony, El Tatio Geyser Field, Chile. *Applied Geochemistry.* **2009**. 24.664-76. Elsevier.

Miller, Jerry R., Paul J. Lechler, Karen A. Hudson-Edwards, and Mark G. Macklin. Lead Isotopic Fingerpriting of Heavy Metal Contamination, Rio Pilcomay Basin, Bolivia. *Geochemistry: Exploration, Environment, Analysis.* **2002**. 2.225-33.

MacDonald DD, Ingersoll CG, Berger TA. Development and evaluation of consensus-based sediment quality guidelines for freshwater ecosystems. *Archives of Environmental Contamination and Toxicology*. **2000.** 39:20-31.

Miller, Jerry R., Suzanne M. Orbock Miller. *Contaminated Rivers*: A Geomorphological-Geochemical Approach to Site Assessment and Remediation New York: Springer, 2007.

Rech, Jason A., Brian S. Currie, Greg Michalski, and Angela M. Cowan. Neogene Climate Change and Uplift in the Atacama Desert, Chile. *Geology*. **2006**. 34.9.761.

Romero, L., P. Campano, L. Fanfani, R. Cidu, C. Dadea, T. Keegan, I. Thornton, and M. Farago. Arsenic Enrichment in Waters and Sediment of the Rio Loa (Second Region Chile). *Applied Geochemistry.* **2003**. 18.1399-416. Pergamon.

Rouxel, Olivier, John Ludden, and Yves Fouquet. Antimony Isotope Variations in Natural Systems and Implications for Their Use as Geochemical Tracers. *Chemical Geology.* **2003**. 200.25-40. Elsevier.

APPENDIX A

t-values calculated for a comparisons of means across basin populations

Pb		
Linear Hypotheses:	t value	Pr(>|t|)
Lower Loa - El Tatio == 0	1.023	0.942
Middle Loa - El Tatio == 0	1	0.948
Mine Tribs - El Tatio == 0	1.554	0.705
Rio Salado - El Tatio == 0	1.269	0.856
Rio San Salvador - El Tatio == 0	1.179	0.893
Upper Loa - El Tatio == 0	2.608	0.16
Middle Loa - Lower Loa == 0	-0.207	1.0000
Mine Tribs - Lower Loa == 0	0.597	0.996
Rio Salado - Lower Loa == 0	0.013	1.0000
Rio San Salvador - Lower Loa == 0	0.049	1.0000
Upper Loa - Lower Loa == 0	1.107	0.918
Mine Tribs - Middle Loa == 0	0.847	0.976
Rio Salado - Middle Loa == 0	0.269	1.0000
Rio San Salvador - Middle Loa == 0	0.285	1.0000
Upper Loa - Middle Loa == 0	1.608	0.672
Rio Salado - Mine Tribs == 0	-0.656	0.994
Rio San Salvador - Mine Tribs == 0	-0.586	0.997
Upper Loa - Mine Tribs == 0	0.291	1.0000
Rio San Salvador - Rio Salado == 0	0.044	1.0000
Upper Loa - Rio Salado == 0	1.339	0.823
Upper Loa - Rio San Salvador == 0	1.154	0.902

As		
Linear Hypotheses:	t value	Pr(>|t|)
Lower Loa - El Tatio == 0	-4.308	0.00352 **
Middle Loa - El Tatio == 0	-4.846	< 0.001 ***
Mine Tribs - El Tatio == 0	-3.704	0.01535 *
Rio Salado - El Tatio == 0	-4.81	0.00103 **
Rio San Salvador - El Tatio == 0	-4.193	0.00493 **
Upper Loa - El Tatio == 0	-5.38	< 0.001 ***
Middle Loa - Lower Loa == 0	0.153	1.0000
Mine Tribs - Lower Loa == 0	0.024	1.0000
Rio Salado - Lower Loa == 0	0.381	0.9997
Rio San Salvador - Lower Loa == 0	0.444	0.99927

Upper Loa - Lower Loa == 0	-0.085	1.0000
Mine Tribs - Middle Loa == 0	-0.107	1.0000
Rio Salado - Middle Loa == 0	0.26	0.99997
Rio San Salvador - Middle Loa == 0	0.34	0.99984
Upper Loa - Middle Loa == 0	-0.283	0.99995
Rio Salado - Mine Tribs == 0	0.303	0.99992
Rio San Salvador - Mine Tribs == 0	0.367	0.99976
Upper Loa - Mine Tribs == 0	-0.1	1.0000
Rio San Salvador - Rio Salado == 0	0.109	1.0000
Upper Loa - Rio Salado == 0	-0.571	0.99703
Upper Loa - Rio San Salvador == 0	-0.619	0.99537

Sb		
Linear Hypothesest value	t value	Pr(>|t|)
Lower Loa - El Tatio == 0	-3.923	0.01088 *
Middle Loa - El Tatio == 0	-4.253	0.00507 **
Mine Tribs - El Tatio == 0	-2.62	0.16275
Rio Salado - El Tatio == 0	-4.789	0.00155 **
Rio San Salvador - El Tatio == 0	-3.905	0.01130 *
Upper Loa - El Tatio == 0	-4.651	0.00231 **
Middle Loa - Lower Loa == 0	0.038	1.0000
Mine Tribs - Lower Loa == 0	-0.048	1.0000
Rio Salado - Lower Loa == 0	0.013	1.0000
Rio San Salvador - Lower Loa == 0	0.016	1.0000
Upper Loa - Lower Loa == 0	-0.058	1.0000
Mine Tribs - Middle Loa == 0	-0.076	1.0000
Rio Salado - Middle Loa == 0	-0.03	1.0000
Rio San Salvador - Middle Loa == 0	-0.021	1.0000
Upper Loa - Middle Loa == 0	-0.106	1.0000
Rio Salado - Mine Tribs == 0	0.06	1.0000
Rio San Salvador - Mine Tribs == 0	0.059	1.0000
Upper Loa - Mine Tribs == 0	0.012	1.0000
Rio San Salvador - Rio Salado == 0	0.005	1.0000
Upper Loa - Rio Salado == 0	-0.085	1.0000
Upper Loa - Rio San Salvador == 0	-0.075	1.0000

Cu		
Linear Hypotheses:	t value	Pr(>|t|)
Lower Loa - El Tatio == 0	-0.215	1.0000
Middle Loa - El Tatio == 0	0.319	0.9999

Mine Tribs - El Tatio == 0	4.576	0.00185 **
Rio Salado - El Tatio == 0	0.057	1.0000
Rio San Salvador - El Tatio == 0	6.575	< 0.001 ***
Upper Loa - El Tatio == 0	0.12	1.0000
Middle Loa - Lower Loa == 0	0.473	0.9990
Mine Tribs - Lower Loa == 0	4.259	0.00422 **
Rio Salado - Lower Loa == 0	0.262	1.0000
Rio San Salvador - Lower Loa == 0	5.756	< 0.001 ***
Upper Loa - Lower Loa == 0	0.308	0.9999
Mine Tribs - Middle Loa == 0	4.235	0.00447 **
Rio Salado - Middle Loa == 0	-0.264	1.0000
Rio San Salvador - Middle Loa == 0	6.039	< 0.001 ***
Upper Loa - Middle Loa == 0	-0.191	1.0000
Rio Salado - Mine Tribs == 0	-4.535	0.00207 **
Rio San Salvador - Mine Tribs == 0	0.587	0.9965
Upper Loa - Mine Tribs == 0	-4.379	0.00309 **
Rio San Salvador - Rio Salado == 0	6.524	< 0.001 ***
Upper Loa - Rio Salado == 0	0.065	1.0000
Upper Loa - Rio San Salvador == 0	-6.219	< 0.001 ***

Sb/Cu		
Linear Hypotheses:	t value	Pr(>|t|)
Lower Loa - El Tatio == 0	-2.984	0.0783
Middle Loa - El Tatio == 0	-3.353	0.0358 *
Mine Tribs - El Tatio == 0	-2.743	0.1271
Rio Salado - El Tatio == 0	-3.802	0.0129 *
Rio San Salvador - El Tatio == 0	-3.465	0.0277 *
Upper Loa - El Tatio == 0	-3.837	0.0115 *
Middle Loa - Lower Loa == 0	-0.071	1.000
Mine Tribs - Lower Loa == 0	-0.142	1.000
Rio Salado - Lower Loa == 0	-0.121	1.000
Rio San Salvador - Lower Loa == 0	-0.166	1.000
Upper Loa - Lower Loa == 0	-0.149	1.000
Mine Tribs - Middle Loa == 0	-0.086	1.000
Rio Salado - Middle Loa == 0	-0.048	1.000
Rio San Salvador - Middle Loa == 0	-0.103	1.000
Upper Loa - Middle Loa == 0	-0.079	1.000
Rio Salado - Mine Tribs == 0	0.054	1.000
Rio San Salvador - Mine Tribs == 0	0.003	1.000
Upper Loa - Mine Tribs == 0	-0.149	1.000

Rio San Salvador - Rio Salado == 0	0.029	1.000
Upper Loa - Rio Salado == 0	-0.035	1.000
Upper Loa - Rio San Salvador == 0	0.033	1.000

Sb-123/Sb-121		
Linear Hypotheses:	t value	Pr(>|t|)
Lower Loa - El Tatio == 0	-1.45	0.76424
Middle Loa - El Tatio == 0	-1.781	0.56464
Mine Tribs - El Tatio == 0	-1.882	0.50262
Rio Salado - El Tatio == 0	-1.485	0.74495
Rio San Salvador - El Tatio == 0	-0.986	0.95065
Upper Loa - El Tatio == 0	3.835	0.01172 *
Middle Loa - Lower Loa == 0	-0.004	1.0000
Mine Tribs - Lower Loa == 0	-0.56	0.99729
Rio Salado - Lower Loa == 0	0.238	0.99998
Rio San Salvador - Lower Loa == 0	0.402	0.99958
Upper Loa - Lower Loa == 0	4.584	0.00193 **
Mine Tribs - Middle Loa == 0	-0.623	0.99516
Rio Salado - Middle Loa == 0	0.296	0.99993
Rio San Salvador - Middle Loa == 0	0.468	0.999
Upper Loa - Middle Loa == 0	5.533	< 0.001 ***
Rio Salado - Mine Tribs == 0	0.832	0.97811
Rio San Salvador - Mine Tribs == 0	0.92	0.96445
Upper Loa - Mine Tribs == 0	4.612	0.00179 **
Rio San Salvador - Rio Salado == 0	0.226	0.99999
Upper Loa - Rio Salado == 0	5.25	< 0.001 ***
Upper Loa - Rio San Salvador == 0	4.134	0.00602 **

Pb-206/Pb-207		
Linear Hypotheses:	t value	Pr(>|t|)
Lower Loa - El Tatio == 0	2	0.431
Middle Loa - El Tatio == 0	0.941	0.961
Mine Tribs - El Tatio == 0	0.032	1.0000
Rio Salado - El Tatio == 0	0.363	1.0000
Rio San Salvador - El Tatio == 0	0.558	0.997
Upper Loa - El Tatio == 0	0.703	0.991
Middle Loa - Lower Loa == 0	-1.232	0.872
Mine Tribs - Lower Loa == 0	-1.521	0.725
Rio Salado - Lower Loa == 0	-1.704	0.613
Rio San Salvador - Lower Loa == 0	-1.38	0.802

Upper Loa - Lower Loa == 0	-1.426	0.778
Mine Tribs - Middle Loa == 0	-0.634	0.995
Rio Salado - Middle Loa == 0	-0.578	0.997
Rio San Salvador - Middle Loa == 0	-0.284	1.0000
Upper Loa - Middle Loa == 0	-0.238	1.0000
Rio Salado - Mine Tribs == 0	0.225	1.0000
Rio San Salvador - Mine Tribs == 0	0.386	1.0000
Upper Loa - Mine Tribs == 0	0.465	0.999
Rio San Salvador - Rio Salado == 0	0.233	1.0000
Upper Loa - Rio Salado == 0	0.34	1.0000
Upper Loa - Rio San Salvador == 0	0.071	1.0000

Pb-206/Pb-208		
Linear Hypotheses:	t value	Pr(>|t|)
Lower Loa - El Tatio == 0	-0.058	1.0000
Middle Loa - El Tatio == 0	-1.343	0.8212
Mine Tribs - El Tatio == 0	-1.46	0.7594
Rio Salado - El Tatio == 0	-0.66	0.9935
Rio San Salvador - El Tatio == 0	-3.311	0.0367 *
Upper Loa - El Tatio == 0	-0.887	0.9704
Middle Loa - Lower Loa == 0	-1.039	0.9379
Mine Tribs - Lower Loa == 0	-1.261	0.8591
Rio Salado - Lower Loa == 0	-0.481	0.9989
Rio San Salvador - Lower Loa == 0	-2.745	0.1232
Upper Loa - Lower Loa == 0	-0.667	0.9931
Mine Tribs - Middle Loa == 0	-0.511	0.9984
Rio Salado - Middle Loa == 0	0.683	0.9922
Rio San Salvador - Middle Loa == 0	-2.11	0.3695
Upper Loa - Middle Loa == 0	0.455	0.9992
Rio Salado - Mine Tribs == 0	0.994	0.9492
Rio San Salvador - Mine Tribs == 0	-1.091	0.9227
Upper Loa - Mine Tribs == 0	0.833	0.9783
Rio San Salvador - Rio Salado == 0	-2.721	0.1288
Upper Loa - Rio Salado == 0	-0.228	1.0000
Upper Loa - Rio San Salvador == 0	2.518	0.1891

Pb-207/Pb-208		
Linear Hypotheses:	t value	Pr(>|t|)

Lower Loa - El Tatio == 0	-0.657	0.9936
Middle Loa - El Tatio == 0	-1.523	0.7232
Mine Tribs - El Tatio == 0	-1.377	0.8042
Rio Salado - El Tatio == 0	-0.735	0.9885
Rio San Salvador - El Tatio == 0	-3.192	0.0481 *
Upper Loa - El Tatio == 0	-1.012	0.9448
Middle Loa - Lower Loa == 0	-0.586	0.9966
Mine Tribs - Lower Loa == 0	-0.722	0.9895
Rio Salado - Lower Loa == 0	0.057	1.0000
Rio San Salvador - Lower Loa == 0	-2.09	0.3807
Upper Loa - Lower Loa == 0	-0.17	1.0000
Mine Tribs - Middle Loa == 0	-0.3	0.9999
Rio Salado - Middle Loa == 0	0.787	0.9836
Rio San Salvador - Middle Loa == 0	-1.83	0.5337
Upper Loa - Middle Loa == 0	0.51	0.9984
Rio Salado - Mine Tribs == 0	0.857	0.975
Rio San Salvador - Mine Tribs == 0	-1.082	0.9257
Upper Loa - Mine Tribs == 0	0.661	0.9934
Rio San Salvador - Rio Salado == 0	-2.534	0.1838
Upper Loa - Rio Salado == 0	-0.277	1.0000
Upper Loa - Rio San Salvador == 0	2.287	0.2815

APPENDIX B

Graphs of pairwise comparisons of means using an ANOVA one way test with 95% confidence.

Pb

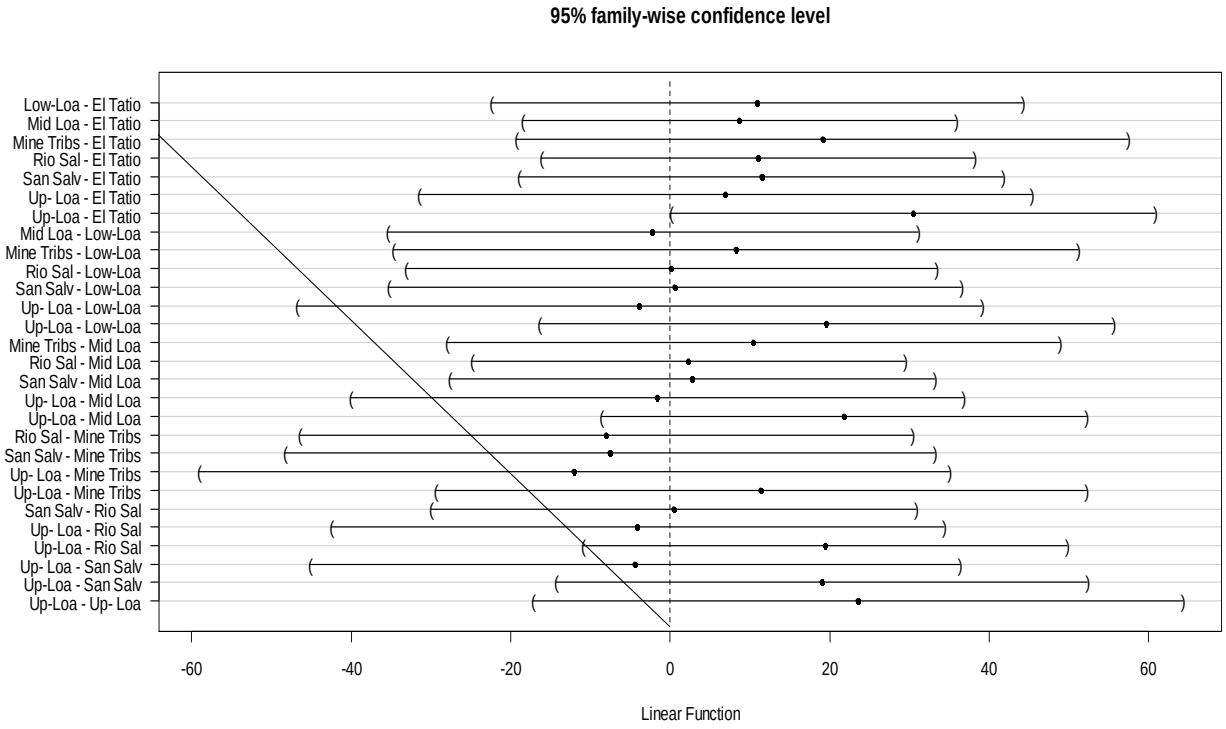

As

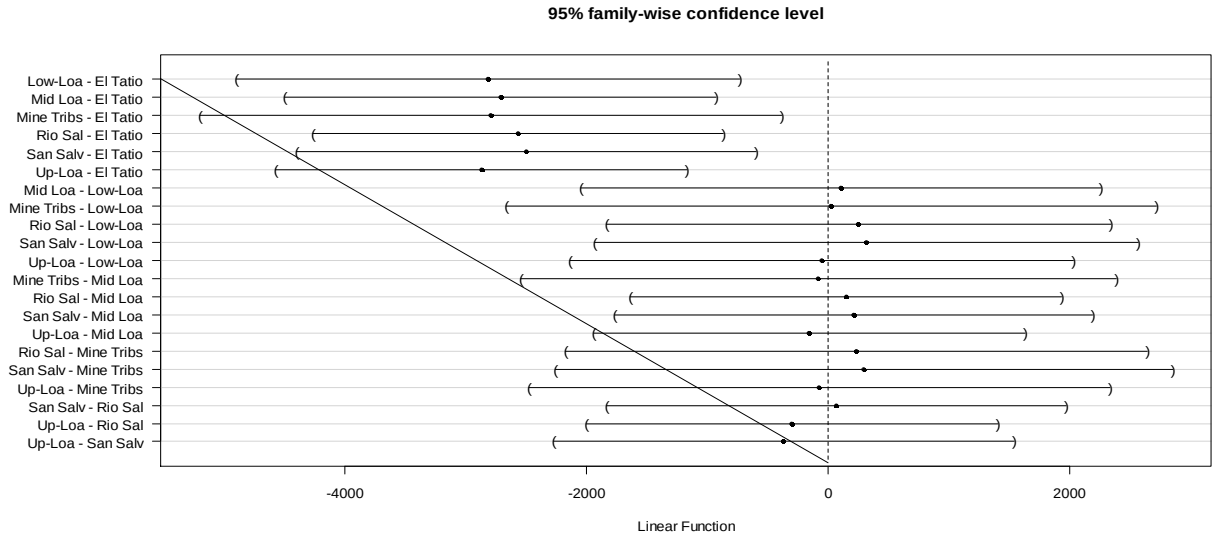

Sb

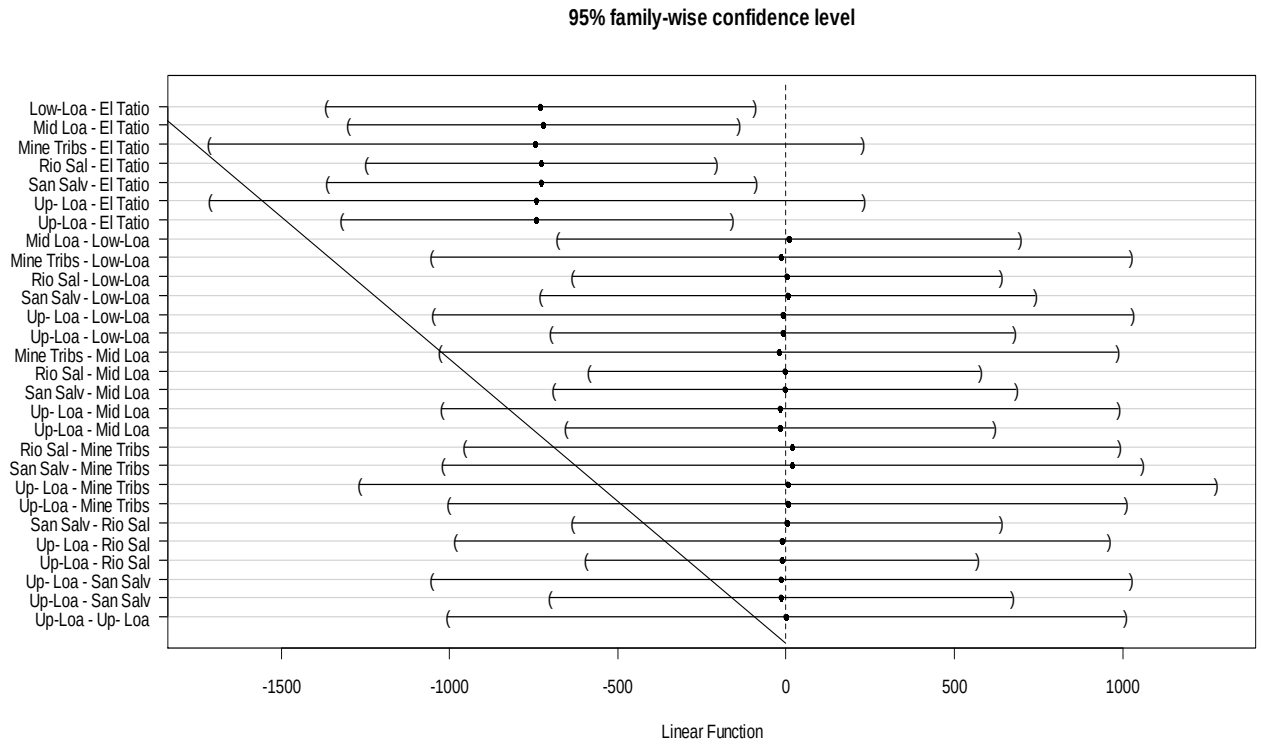
95% family-wise confidence level
Low-Loa - El Tatio
Mid Loa - El Tatio
Mine Tribs - El Tatio
Rio Sal - El Tatio
San Salv - El Tatio
Up- Loa - El Tatio
Up-Loa - El Tatio
Mid Loa - Low-Loa
Mine Tribs - Low-Loa
Rio Sal - Low-Loa
San Salv - Low-Loa
Up- Loa - Low-Loa
Up-Loa - Low-Loa
Mine Tribs - Mid Loa
Rio Sal - Mid Loa
San Salv - Mid Loa
Up- Loa - Mid Loa
Up-Loa - Mid Loa
Rio Sal - Mine Tribs
San Salv - Mine Tribs
Up- Loa - Mine Tribs
Up-Loa - Mine Tribs
San Salv - Rio Sal
Up- Loa - Rio Sal
Up-Loa - Rio Sal
Up- Loa - San Salv
Up-Loa - San Salv
Up-Loa - Up- Loa
-1500
-1000
-500
0
500
1000
Linear Function

Cu

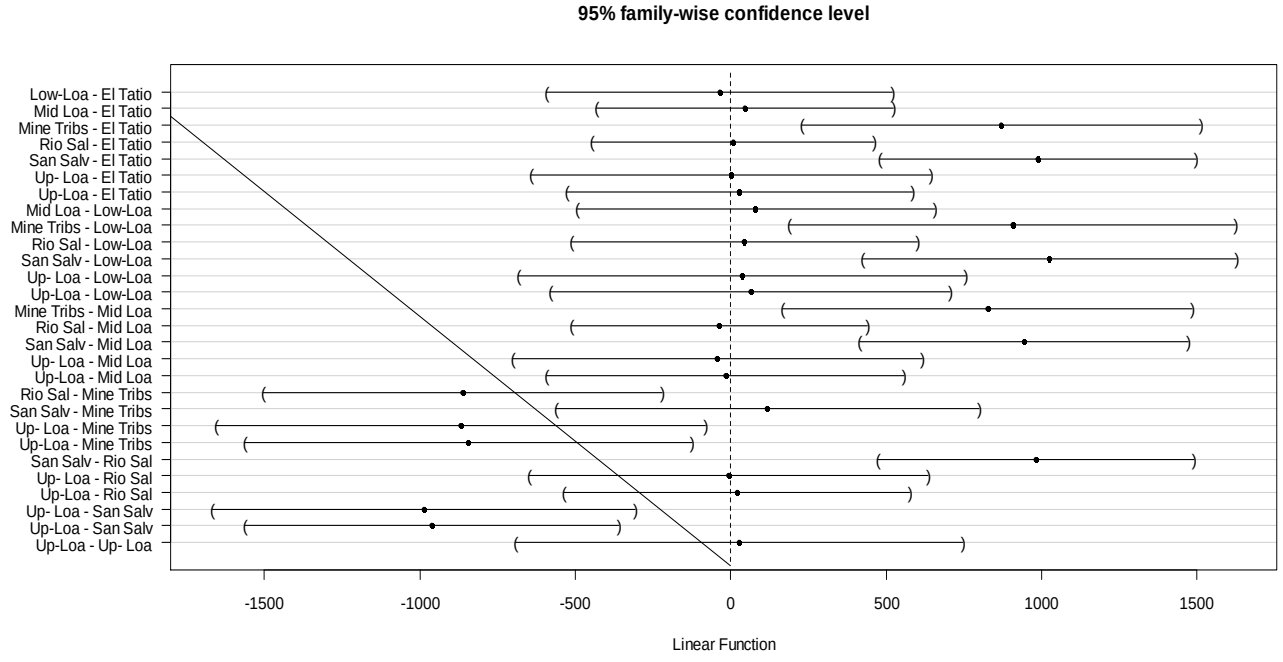
95% family-wise confidence level
Low-Loa - El Tatio
Mid Loa - El Tatio
Mine Tribs - El Tatio
Rio Sal - El Tatio
San Salv - El Tatio
Up- Loa - El Tatio
Up-Loa - El Tatio
Mid Loa - Low-Loa
Mine Tribs - Low-Loa
Rio Sal - Low-Loa
San Salv - Low-Loa
Up- Loa - Low-Loa
Up-Loa - Low-Loa
Mine Tribs - Mid Loa
Rio Sal - Mid Loa
San Salv - Mid Loa
Up- Loa - Mid Loa
Up-Loa - Mid Loa
Rio Sal - Mine Tribs
San Salv - Mine Tribs
Up- Loa - Mine Tribs
Up-Loa - Mine Tribs
San Salv - Rio Sal
Up- Loa - Rio Sal
Up-Loa - Rio Sal
Up- Loa - San Salv
Up-Loa - San Salv
Up-Loa - Up- Loa
-1500
-1000
-500
0
500
1000
1500
Linear Function

Sb/Cu

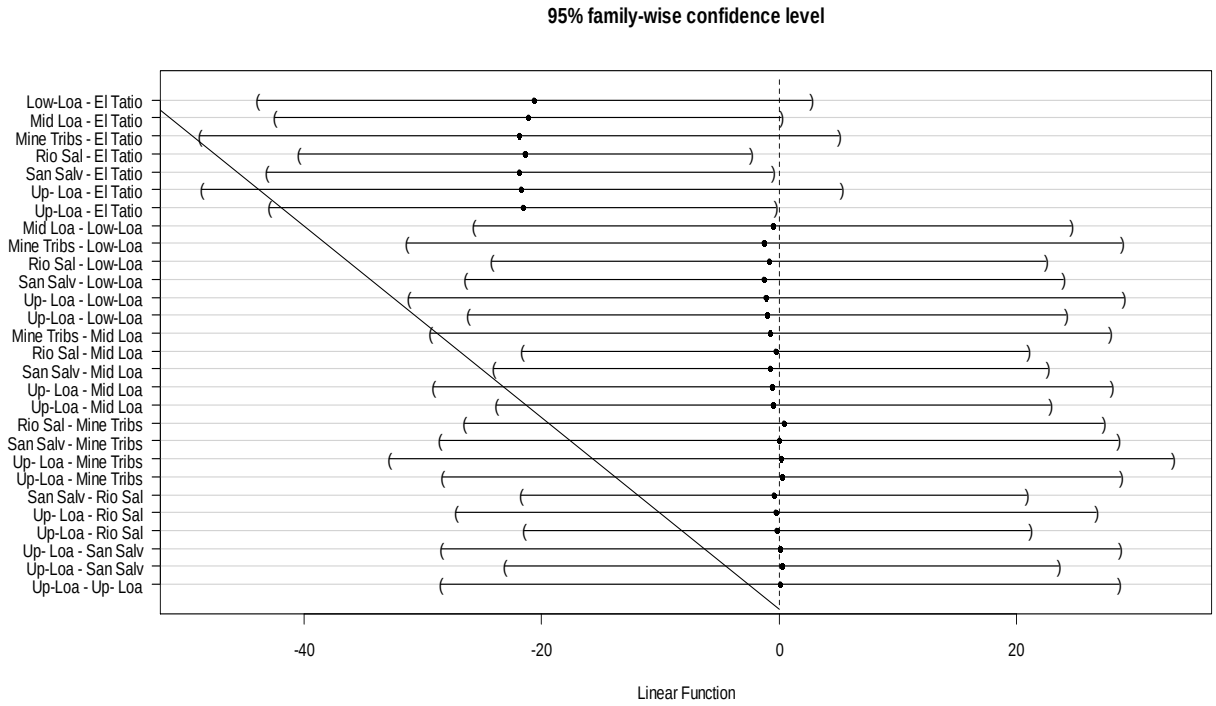
95% family-wise confidence level
Low-Loa - El Tatio
Mid Loa - El Tatio
Mine Tribs - El Tatio
Rio Sal - El Tatio
San Salv - El Tatio
Up- Loa - El Tatio
Up-Loa - El Tatio
Mid Loa - Low-Loa
Mine Tribs - Low-Loa
Rio Sal - Low-Loa
San Salv - Low-Loa
Up- Loa - Low-Loa
Up-Loa - Low-Loa
Mine Tribs - Mid Loa
Rio Sal - Mid Loa
San Salv - Mid Loa
Up- Loa - Mid Loa
Up-Loa - Mid Loa
Rio Sal - Mine Tribs
San Salv - Mine Tribs
Up- Loa - Mine Tribs
Up-Loa - Mine Tribs
San Salv - Rio Sal
Up- Loa - Rio Sal
Up-Loa - Rio Sal
Up- Loa - San Salv
Up-Loa - San Salv
Up-Loa - Up- Loa
-40
-20
0
20
Linear Function

Sb-123/Sb-121

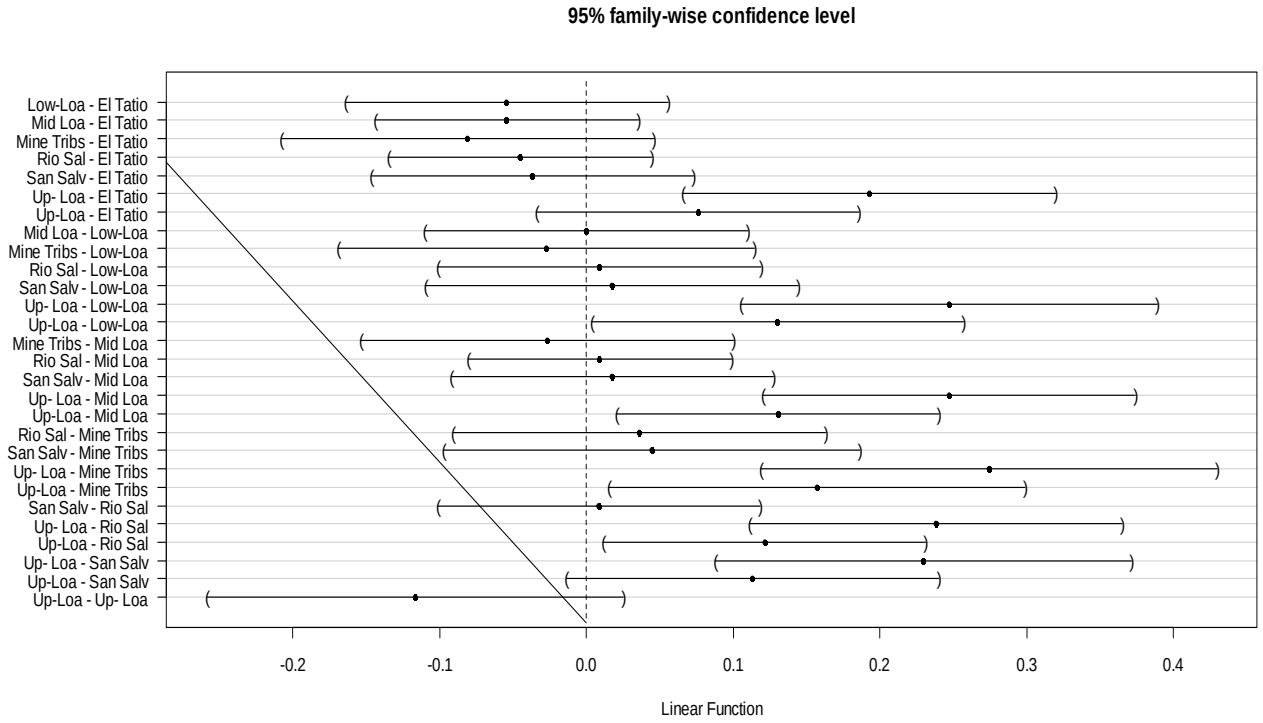
95% family-wise confidence level
Low-Loa - El Tatio
Mid Loa - El Tatio
Mine Tribs - El Tatio
Rio Sal - El Tatio
San Salv - El Tatio
Up- Loa - El Tatio
Up-Loa - El Tatio
Mid Loa - Low-Loa
Mine Tribs - Low-Loa
Rio Sal - Low-Loa
San Salv - Low-Loa
Up- Loa - Low-Loa
Up-Loa - Low-Loa
Mine Tribs - Mid Loa
Rio Sal - Mid Loa
San Salv - Mid Loa
Up- Loa - Mid Loa
Up-Loa - Mid Loa
Rio Sal - Mine Tribs
San Salv - Mine Tribs
Up- Loa - Mine Tribs
Up-Loa - Mine Tribs
San Salv - Rio Sal
Up- Loa - Rio Sal
Up-Loa - Rio Sal
Up- Loa - San Salv
Up-Loa - San Salv
Up-Loa - Up- Loa
-0.2
-0.1
0.0
0.1
0.2
0.3
0.4
Linear Function

Pb-206/Pb-207

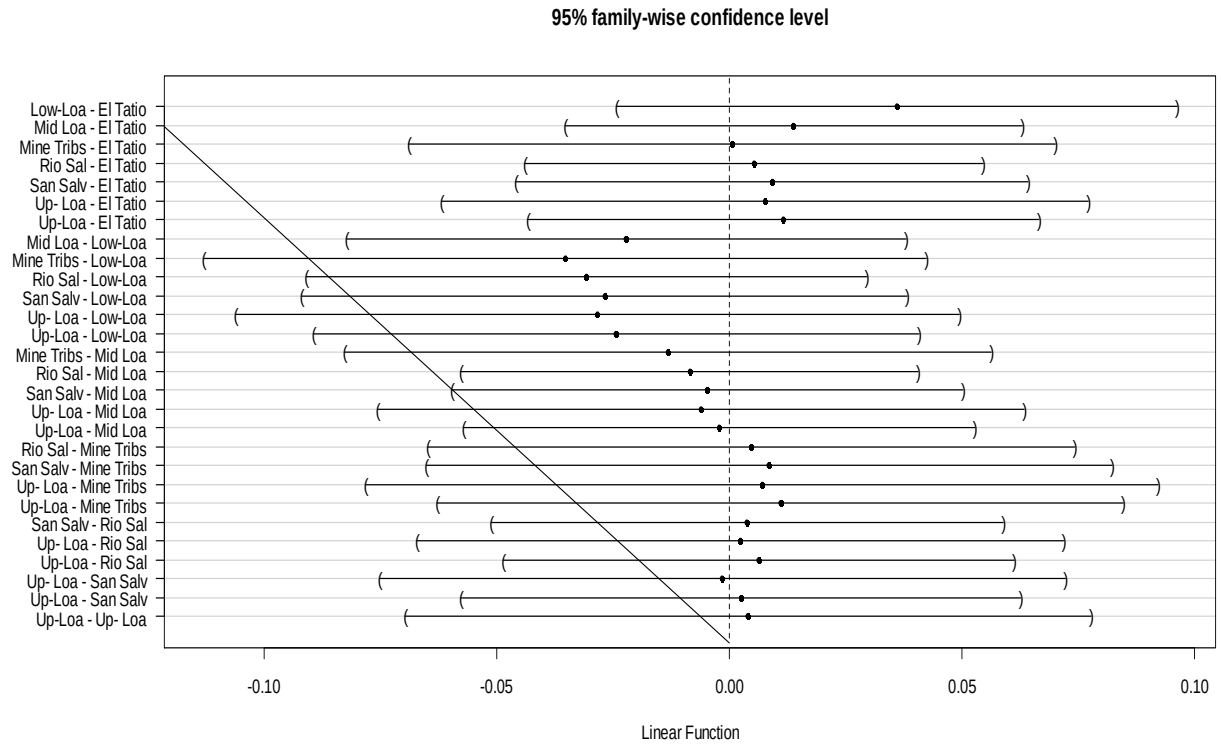

Pb-206/Pb-208

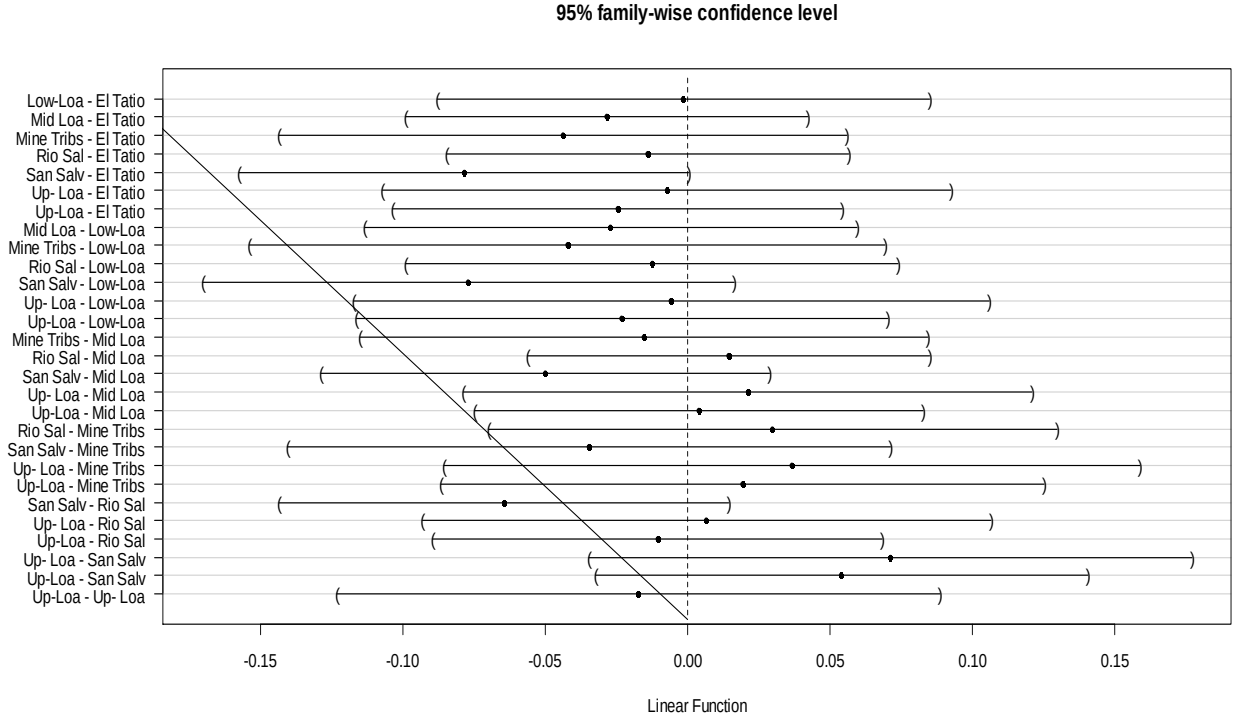

Pb-207/Pb-208

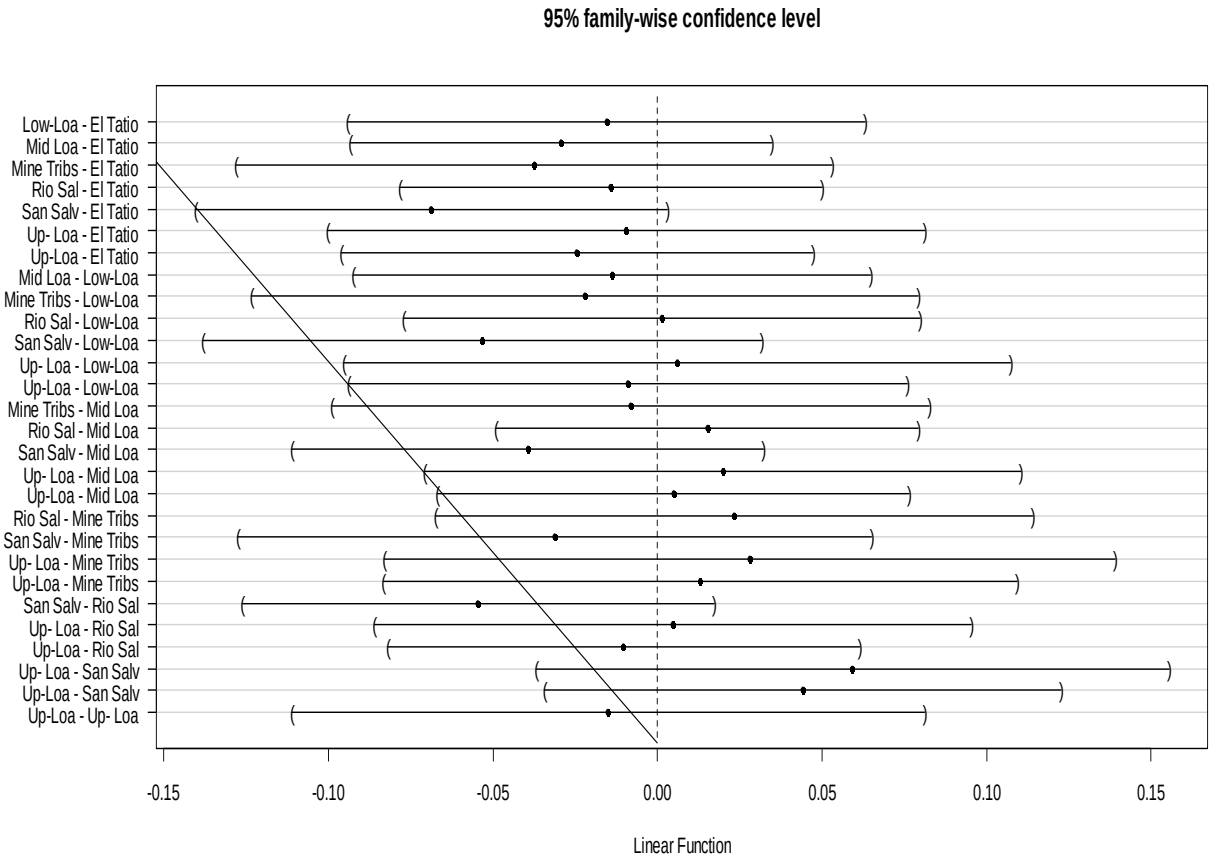
95% family-wise confidence level
Low-Loa - El Tatio
Mid Loa - El Tatio
Mine Tribs - El Tatio
Rio Sal - El Tatio
San Salv - El Tatio
Up- Loa - El Tatio
Up-Loa - El Tatio
Mid Loa - Low-Loa
Mine Tribs - Low-Loa
Rio Sal - Low-Loa
San Salv - Low-Loa
Up- Loa - Low-Loa
Up-Loa - Low-Loa
Mine Tribs - Mid Loa
Rio Sal - Mid Loa
San Salv - Mid Loa
Up- Loa - Mid Loa
Up-Loa - Mid Loa
Rio Sal - Mine Tribs
San Salv - Mine Tribs
Up- Loa - Mine Tribs
Up-Loa - Mine Tribs
San Salv - Rio Sal
Up- Loa - Rio Sal
Up-Loa - Rio Sal
Up- Loa - San Salv
Up-Loa - San Salv
Up-Loa - Up- Loa
-0.15
-0.10
-0.05
0.00
0.05
0.10
0.15
Linear Function